European Journal of Medicinal Chemistry 69 (2013) 399–412

Contents lists available at ScienceDirect

European Journal of Medicinal Chemistry

journal homepage: http://www.elsevier.com/locate/ejmech

Original article

Design, synthesis, and biological evaluation of novel 2-ethyl-5-phenylthiazole-4-carboxamide derivatives as protein tyrosine phosphatase 1B inhibitors with improved cellular efficacy

Yue-Ting Chen [1], Chun-Lan Tang [1], Wei-Ping Ma, Li-Xin Gao, Yi Wei, Wei Zhang, Jing-Ya Li**, Jia Li**, Fa-Jun Nan*

Chinese National Center for Drug Screening, State Key Laboratory of Drug Research, Shanghai Institute of Materia Medica, Chinese Academy of Sciences, 189 Guoshoujing Road, Zhangjiang Hi-Tech Park, Shanghai 201203, People's Republic of China

ARTICLE INFO

Article history:
Received 5 April 2013
Received in revised form
6 August 2013
Accepted 10 September 2013
Available online 19 September 2013

Keywords:
Protein tyrosine phosphatase 1B
Type 2 diabetes
2-Ethyl-5-phenylthiazole-4-carboxamide (PTA)
SAR

ABSTRACT

Protein tyrosine phosphatase 1B (PTP1B) is implicated as a key negative regulator of the insulin and leptin signal-transduction pathways. PTP1B inhibitors have emerged as attractive and potent pharmaceutical agents for the treatment of type 2 diabetes and obesity. We identified a series of 2-ethyl-5-phenylthiazole-4-carboxamide (PTA) derivatives, inspired from the ACT scaffold of Scleritodermin A, as a novel class of PTP1B inhibitors. Structure–activity relationship (SAR) analysis and docking studies revealed the molecular basis of PTP1B inhibition by these compounds. PTA derivative **18g** was capable of inhibiting intracellular PTP1B and subsequently activating the insulin signaling pathway. Treatment of cells with **18g** markedly increased the phosphorylation levels of IRβ and Akt as well as the rate of glucose uptake.

1. Introduction

Type 2 diabetes and obesity are characterized by resistance to the hormones insulin and leptin [1]. Impaired insulin and leptin signaling play a key role in the pathogenesis of type 2 diabetes. Protein tyrosine phosphatase 1B (PTP1B) is an intracellular non-receptor phosphatase (PTPase) that is implicated as a key negative regulator in signal transduction for both insulin [2–4] and leptin [5–9] pathways. It acts by dephosphorylating specific phosphotyrosine (pTyr) residues of the insulin receptor (IR) [10–12], IR substrates (IRS) [13] and Janus kinase 2 (JAK2) [14,15]. PTP1B expression and activity are increased in pathologically insulin-resistant and obese humans [16–18]. In two landmark PTP1B knockout studies, PTP1B-deficient mice displayed increased insulin sensitivity and resistance to diet-induced obesity [19,20]. Consistent with this finding, diabetic mice treated with specific PTP1B antisense oligonucleotides exhibited normalized blood glucose level, improved insulin sensitivity and modulated fat storage and lipogenesis in adipose tissue [21,22]. Therefore, PTP1B inhibitors have emerged as attractive and potent pharmaceutical agents and may provide a novel strategy for the treatment of type 2 diabetes and obesity [23–25].

Various PTP1B inhibitors have been developed over the past decade. Some compounds display high binding affinity, but many do not show inhibitory potency against intracellular PTP1B. Because of the highly cationic character of the active site of PTP1B enzyme, most pTyr mimetics are negatively charged at physiological pH, and this highly polar nature provides these compounds with poor physiochemical properties and therefore poor cell permeability and low oral bioavailability. Although developing potent and specific PTP1B inhibitors with high cell permeability and orally bioavailability remains challenging, there are a number of examples of PTP1B inhibitors with cellular and/or in vivo activity, which may lead to opportunities to develop new treatment strategies for type 2 diabetes and obesity [26–30].

We previously reported our discovery of novel PTP1B inhibitors with an ACT (2-(1-amino-2-*p*-hydroxyphenylethane)-4-(4-carboxy-2,4-dimethyl-2*Z*,4*E*-propadiene)-thiazole) skeleton [31] inspired by the key structure of the natural product

* Corresponding author. Fax: +86 21 50800954.
** Corresponding authors. Fax: +86 21 50801552.
E-mail addresses: jyli@mail.shcnc.ac.cn (J.-Y. Li), jli@mail.shcnc.ac.cn (J. Li), fjnan@mail.shcnc.ac.cn (F.-J. Nan).
[1] These authors contributed equally to this work.

0223-5234/$ – see front matter © 2013 Elsevier Masson SAS. All rights reserved.
http://dx.doi.org/10.1016/j.ejmech.2013.09.017

Scleritodermin A [32]. Structural modification at sites A, B, and C (R^1, R^2 and R^3), and the conjugated diene moiety (Fig. 1) led to a series of ACT derivatives with improved inhibitory activity (low micromolar IC_{50} value) compared with the original hit and moderate selectivity over TCPTP. In this study, considering the reactive properties of the conjugated diene ester moiety as a Michael acceptor and the difficulties of synthesis, we carried out further structural optimization to replace the conjugated diene moiety. And also several substituent groups were introduced to the C5 position of the thiazole moiety (site D) to investigate the role of site D in PTP1B inhibitory activity. We focused on site D and the conjugated diene moiety (Fig. 1), and subsequently identified a series of 2-ethyl-5-phenylthiazole-4-carboxamide (PTA) derivatives as PTP1B inhibitors with improved in vitro efficacy.

2. Chemistry

The synthesis of the ACT-diene derivatives was performed as shown in Scheme 1. Boc-L-Tyr(Bn)-OH was reacted with $R_4C(O)CH(NH_2)COOEt$ to give amides **2a**–**c**. A thiazole ring was then constructed using Lawesson's reagent to obtain intermediates **3a**–**c**. The conjugated double bonds were constructed via Horner–Wadsworth–Emmons reaction and Still–Gennari phosphonate reaction after converting the ester groups of **3a**–**c** and **6a**–**c** to aldehyde groups (**5a**–**c** and **7a**–**c**) with $LiAlH_4$ and IBX, respectively. The resulting ACT derivatives **8a**–**c** were deprotected using TFA/CH_2Cl_2 and then reacted with cyclohexanecarbonyl chloride to furnish the desired analogs **9a**–**c**.

The synthesis of 2-ethylthiazole-4-carboxamide derivatives commenced with removal of the Boc group of intermediate **10**, followed by acylation with cyclohexanecarbonyl chloride to afford amide **12**. Compound **12** was hydrolyzed to afford the corresponding acid **13**. Condensation of acid **13** and methyl aminobenzoates afforded amides **14a**–**c**, which were then hydrolyzed to afford acids **14d**–**f** (Scheme 2).

The PTA derivatives **17a**, **b** and **18a**, **b** were synthesized as shown in Scheme 3. Intermediate **3c** was hydrolyzed and then reacted with methyl 3-aminobenzoate hydrochloride to afford amide **16**. The Boc group of amide **16** was deprotected by 4 M HCl/EtOAc, and the resulting amine was reacted with cyclohexanecarbonyl chloride or 3-indolepropionic acid to afford compound **17a** and **18a**. Acid **17b** and **18b** were then obtained via hydrolysis of ester **17a** or **18a** with LiOH.

Furthermore, in order to determine the effect of the substitutions on the phenyl ring at site C, compounds **18c**–**n** were synthesized as shown in Scheme 4. Deprotection of the Boc-protected amine **3c** with TFA afforded amine **19**. Amine **19** was reacted with 3-indolepropionic acid and then hydrolyzed to afford acid **21**. Acid **21** reacted with several substituted methyl aminobenzoates followed by hydrolysis to afford various PTA derivatives **18c**–**n**.

3. Results and discussion

3.1. Structure–activity relationship

Structure–activity relationship studies, focused on site D and the conjugated diene moiety, were carried out based on our previous work [31]. First, to investigate the role of site D in the ACT skeleton, several substituent groups were introduced to the C5 position of the thiazole moiety to afford compounds **9a**–**d**. The C5 position of the thiazole moiety was tolerant to several substituents (Table 1). Introduction of bulky substituents retained PTP1B inhibitory activity. The isobutyl derivative **9b** (IC_{50} 9.54 ± 1.99 μM) and the phenyl derivative **9c** (IC_{50} 8.44 ± 1.68 μM) exhibited similar inhibitory activity to the unsubstituted analog **1a** (IC_{50} 9.32 ± 0.42 μM) [31], while the methyl derivative **9a** (IC_{50} 13.46 ± 1.95 μM) displayed slightly decreased inhibitory activity. Compounds **1a** and **9c** were then hydrolyzed to give acids **1b** and **9d**, respectively. Both acids displayed similar potency (IC_{50} 14.69 ± 1.16 μM and 10.89 ± 1.08 μM for **1b** and **9d**, respectively) compared to their corresponding esters (IC_{50} 9.32 ± 0.42 μM and 8.44 ± 1.68 μM for **1a** and **9c**, respectively).

In our previous research, we found that the thiazole-derived conjugated diene moiety was essential for inhibitory activity against PTP1B and the *cis*–*trans* isomers retained the activities. This result allowed us to replace the conjugated diene moiety with an aryl group by considering its instability as a Michael acceptor and the long synthetic route of constructing the conjugated double bonds. Therefore, a series of 2-ethylthiazole-4-carboxamide derivatives (Fig. 1) were synthesized as the analogs of ACT derivatives **1a**, **b**. As shown in Table 2, all the 2-ethylthiazole-4-carboxamide

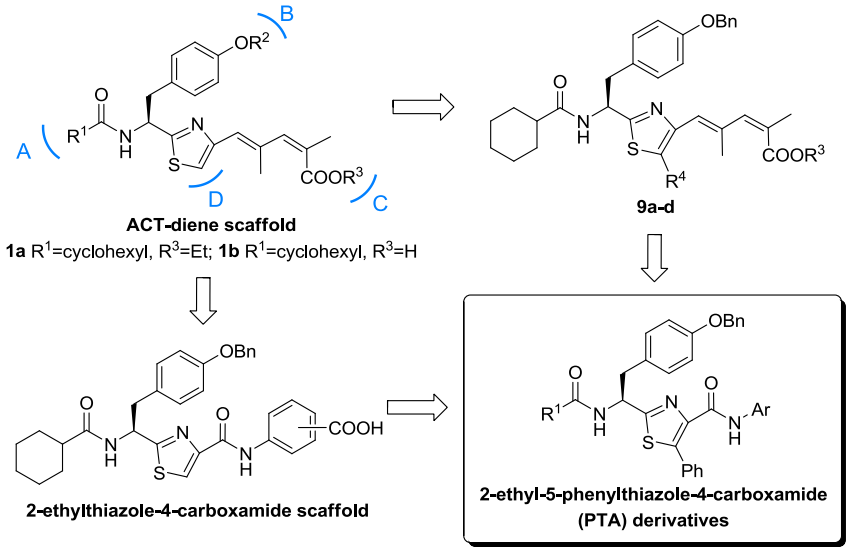

Fig. 1. Structural optimization of PTP1B inhibitors inspired from the ACT scaffold.

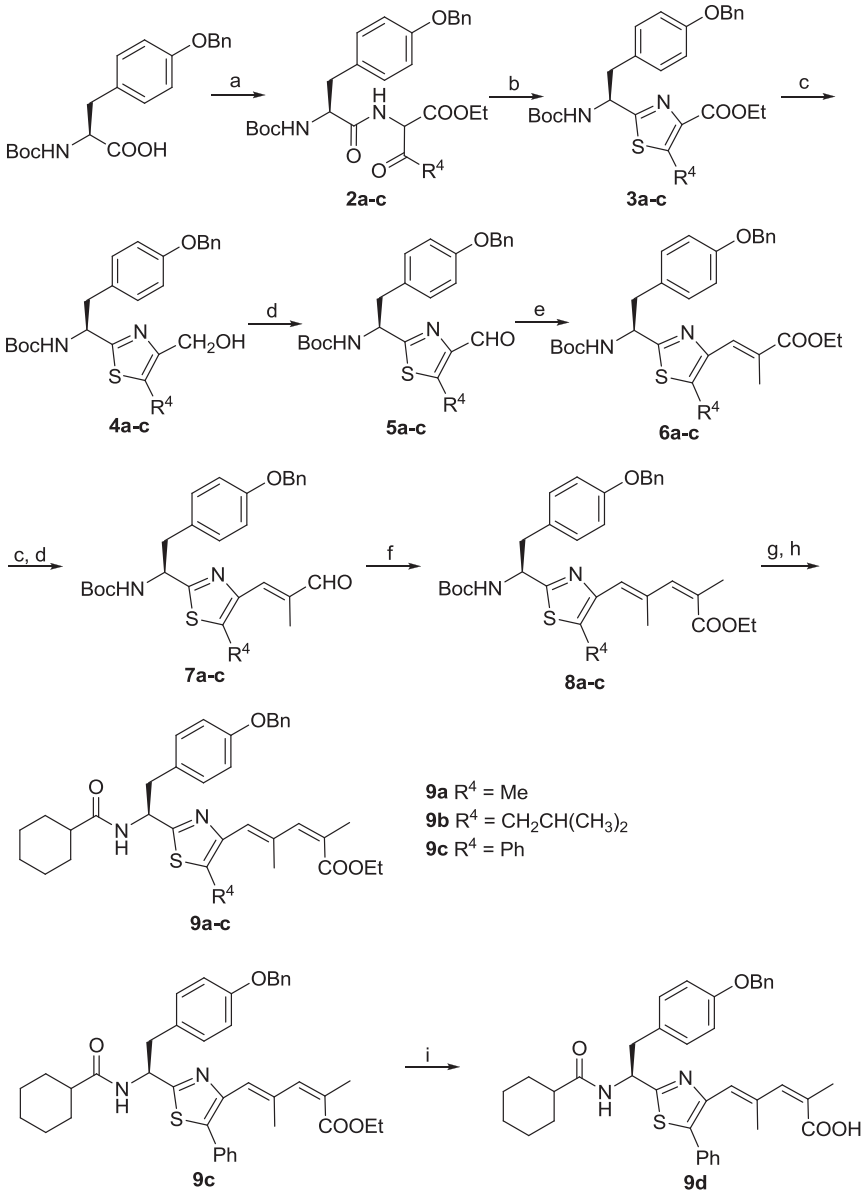

Scheme 1. Reagents and conditions: (a) $R^4C(O)CH(NH_2)COOEt$, EDCI, DMAP, Et_3N, CH_2Cl_2; (b) Lawesson's reagent, THF, reflux; (c) $LiAlH_4$, THF, 0 °C; (d) IBX, DMSO, toluene; (e) $(EtO)_2P(O)CH(CH_3)COOEt$, NaH, THF, 0 °C → rt; (f) $(CF_3CH_2O)_2P(O)CH(CH_3)COOEt$, KHMDS, 18-crown-6, THF, −78 °C; (g) TFA, CH_2Cl_2; (h) cyclohexanecarbonyl chloride, DIPEA, CH_2Cl_2, rt; (i) $LiOH \cdot H_2O$, 1,4-dioxane/H_2O, reflux.

derivatives (**14a**–**f**) displayed moderate PTP1B inhibitory activities, which demonstrated that replacing the conjugated diene moiety with an aryl group could lead to retention of the inhibitory activity. The *ortho*- and *para*-carboxyl-substituted analogs **14d** and **f** (IC_{50} 8.12 ± 0.98 μM and 4.88 ± 0.60 μM, respectively) showed similar inhibitory activity to their corresponding esters **14a** and **c** (IC_{50} 8.79 ± 1.60 μM and 4.42 ± 0.85 μM, respectively). However, the *meta*-carboxyl-substituted analogs **14e** (IC_{50} 6.00 ± 0.43 μM) displayed slightly improvement compared with its corresponding ester **14b** (IC_{50} 10.55 ± 1.48 μM). Comparing the two skeletons, the 2-ethylthiazole-4-carboxamide derivatives **14c**, **e**, and **f** (IC_{50} 4.42 ± 0.85 μM, 6.00 ± 0.43 μM and 4.88 ± 0.60 μM, respectively) exhibited lower IC_{50} values than the ACT derivatives **1a** and **b** (IC_{50} 9.32 ± 0.42 μM and 14.69 ± 1.16 μM, respectively).

Given the observed inhibitory activity of both ACT and 2-ethylthiazole-4-carboxamide derivatives, we proceeded to assess their capacity to inhibit intracellular PTP1B. PTP1B has been reported to act as a negative regulator of the insulin signaling pathway through the dephosphorylation of the IR. Hence, inhibition of PTP1B activity should enhance insulin action and signaling. The above compounds were tested in Chinese hamster ovary cells overexpressing the human IR (CHO-hIR), and IR phosphorylation in whole-cell lysates was examined by western blot analysis. Both the ACT and 2-ethylthiazole-4-carboxamide derivatives were investigated, but only acid **9d**, which has a phenyl group substituted at the C5 position of the thiazole moiety, increased IR phosphorylation weakly in CHO-hIR cells (as shown in Fig. 2a). All the C5-unsubstituted analogs, including the ACT derivatives and 2-ethylthiazole-4-carboxamide derivatives, lacked cellular efficacy. Acid **9d** demonstrated a slight increase in IR phosphorylation in the concentration range of 1.25–10 μM. Notably, the inhibitory concentration values against intracellular PTP1B of compound **9d** and its IC_{50} value observed in the enzyme assay were of an equal order of magnitude. By contrast, quite a few PTP1B inhibitors lack cellular

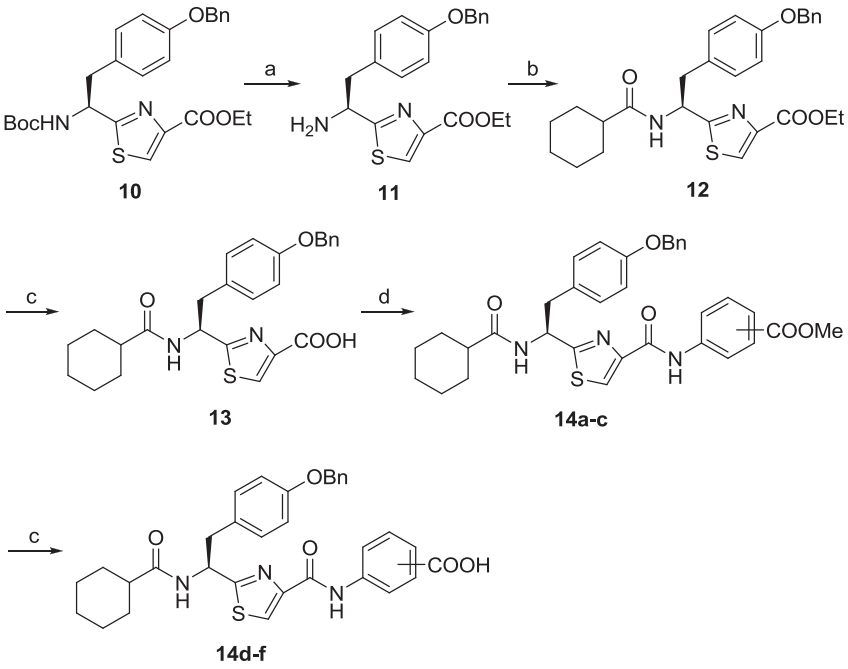

Scheme 2. Reagents and conditions: (a) TFA, CH_2Cl_2, 0 °C → rt; (b) cyclohexanecarbonyl chloride, DIPEA, CH_2Cl_2; (c) LiOH·H_2O, 1,4-dioxane/H_2O; (d) $H_2NC_6H_4COOMe$·HCl, EDCI, DMAP, Et_3N, CH_2Cl_2, rt.

efficacy because of their poor membrane permeability [27]. This result indicated that compound **9d** was membrane permeable and capable of blocking PTP1B activity in cells. However, its analogs, ACT derivatives **1a**, **b** and 2-ethylthiazole-4-carboxamide derivatives **14a**–**f** were devoid of cellular efficacy. This result implied that the introduction of a phenyl group at the C5 position of the thiazole moiety improved the membrane permeability of the ACT derivatives and improved their cellular efficacy.

Although compounds **14a**–**f** lacked cellular efficacy compared with the ACT-diene skeleton, these compounds could be synthesized easily via a simple amidation of substituted thiazole-4-carboxylic acid with amines. Hence, we decided to focus our efforts on further structural modification based on the 2-ethylthiazole-4-carboxamide skeleton. To improve the cellular activities, a phenyl group was introduced onto the C5 position of the thiazole ring, which afforded the 2-ethyl-5-phenylthiazole-4-carboxamide (PTA) skeleton, to give compound **17b** as the analog of acid **14e**. As shown in Table 3, ester **17a** (IC_{50} 3.79 ± 0.67 μM) was twice as potent as the ACT and 2-ethylthiazole-4-carboxamide analogs (esters **9c** and **14b**, IC_{50} 8.44 ± 1.68 μM and 10.55 ± 1.48 μM, respectively). The corresponding acid **17b** (IC_{50} 1.17 ± 0.09 μM) showed a 5.1- to 9.3-fold increase in potency compared with its analogs **9d** and **14e** (IC_{50} 10.89 ± 1.08 μM and 6.00 ± 0.43 μM, respectively). This improvement in inhibitory activity encouraged us to try to further optimize the structure of the PTA scaffold. In our previous report, the 2-(1*H*-indol-3-yl)-ethyl derivatives showed preferable inhibitory activity compared with its analogs [31]. Hence, we induced the 2-(1*H*-indol-3-yl) ethyl group to the PTA scaffold to give ester **18a** and acid **18b**, both of which displayed low micromolar IC_{50} values against PTP1B (IC_{50} 2.68 ± 0.18 μM for **18a** and 1.01 ± 0.07 μM for **18b**). These results demonstrated the feasibility of introducing a phenyl group to the

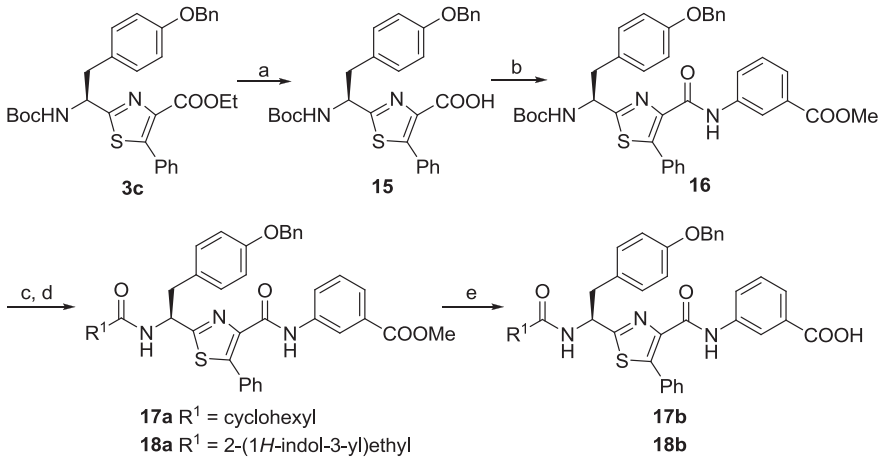

Scheme 3. Reagents and conditions: (a) LiOH·H_2O, THF/H_2O, 50 °C; (b) methyl 3-aminobenzoate hydrochloride, HATU, NMM, CH_2Cl_2; (c) 4 M HCl/EtOAc; (d) cyclohexanecarbonyl chloride, Et_3N, CH_2Cl_2; or 3-indolepropionic acid, EDCI, DMAP, CH_2Cl_2, rt; (e) LiOH·H_2O, THF/MeOH/H_2O.

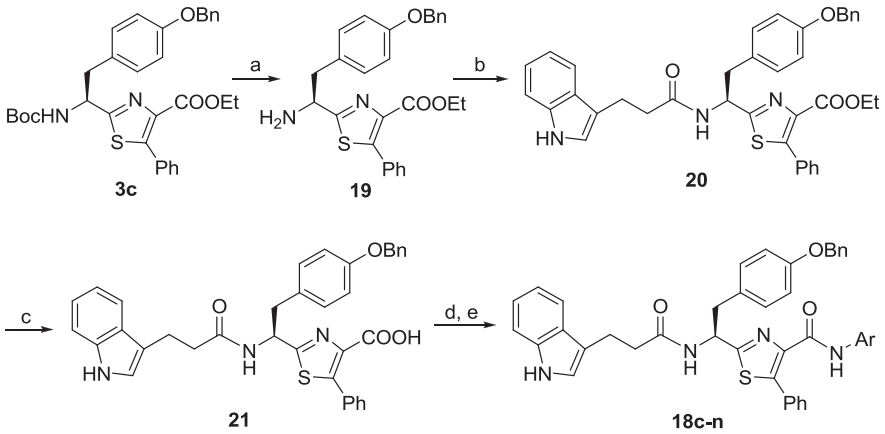

Scheme 4. Reagents and conditions: (a) TFA, CH_2Cl_2, 0 °C → rt; (b) 3-indolepropionic acid, EDCI, DMAP, CH_2Cl_2, rt; (c) K_2CO_3, MeOH/H_2O, rt; (d) $ArNH_2$, HATU, NMM, CH_2Cl_2; (e) LiOH·H_2O, THF/MeOH/H_2O.

C5 position of the thiazole ring of the 2-ethylthiazole-4-carboxamide scaffold because all the resulting PTA derivatives retained inhibitory activity against PTP1B.

The 2-(1*H*-indol-3-yl)-ethyl-substituted acid **18b** emerged as the most potent PTP1B inhibitor among all of the compounds mentioned above. To determine whether the inhibitory effect of PTA derivatives observed in the PTP1B enzyme assay could be recapitulated in a cellular assay, we tested these compounds in CHO-hIR and examined IR phosphorylation by western blot analysis. As shown in Fig. 2b, acid **18b** in the low micromolar range (5–20 μM) elicited a concentration-dependent increase in IR phosphorylation level. However, its corresponding ester **18a** was inactive in cells. Compared with acid **9d** as a closely related control, compound **18b** was more effective in stimulating IR phosphorylation. These results suggested that PTA derivative **18b** possessed improved cell permeability and could stimulate the insulin signaling pathway in cells. These results confirmed our hypothesis and the feasibility of introducing a phenyl group to the C5 position of the thiazole ring to improve the membrane permeability and cellular efficacy of the ACT-derived compounds.

After confirming the cellular efficacy of the PTA skeleton, we continued further structural modification by changing the substitution position of the carboxyl group or by introducing a halogen to the phenyl ring at site C to afford compounds **18c**–**n**. As shown in Table 4, either *ortho*- or *para*-carboxyl-substituted analogs (**18c** and **18d**, IC_{50} 5.56 ± 0.68 μM and 2.28 ± 0.67 μM, respectively) showed less potency than the *meta*-carboxyl-substituted analog **18b** (IC_{50} 1.01 ± 0.07 μM). The introduction of halogen atoms caused different effects on these three acids. Halogen substitution at the 5-position of the 2-carboxyl analog led to a 5- to 10-fold increase in inhibitory activity (**18g**–**i**, IC_{50} 0.54 ± 0.18 μM, 0.71 ± 0.11 μM, and 1.18 ± 0.21 μM, respectively) compared with the parent compound **18c** (IC_{50} 5.56 ± 0.68 μM). Both fluorinated and chlorinated analogs (**18g** and **h**) displayed submicromolar IC_{50} values against PTP1B. The introduction of strong electron-withdrawing F and Cl atoms in the para position of the carboxyl group lowers the pKa values of compounds **18g** and **h**, which provides more favorable interactions with the highly cationic phosphatase active site of PTP1B. The 4-carboxy-2-fluoro-substituted analog **18m**, with a submicromolar IC_{50} value (IC_{50} 0.77 ± 0.12 μM), also exhibited increased enzyme inhibitory activity compared with the corresponding nonhalogenated acid **18d** (IC_{50} 2.28 ± 0.67 μM).

These results reveal some interesting structure–activity relationships for PTP1B inhibition by PTA derivatives. Introduction of a phenyl group at the C5 position of the thiazole moiety benefits the inhibitory activity, membrane permeability and cellular efficacy. Halogen substitutions on the right-hand phenyl ring also affect the potency of compounds; 2-carboxy-5-fluoro-substitution appeared to be the best.

3.2. Selectivity against other phosphatases

The PTPase domains of all PTPases are highly conserved. T-cell protein tyrosine phosphatase (TCPTP), the most homologous phosphatase to PTP1B, has 74% sequence identity in the catalytic domain. TCPTP knockout mice are born healthy but die at 3–5 weeks of age because of impaired B cell and T cell function [33]. While heterozygous deficiency of TCPTP doesn't result in any overt immune phenotype [33] and may be beneficial in the context of type 2 diabetes, as TCPTP is also an important regulator of insulin

Table 1
PTP1B inhibition data for compounds **1a**, **b** and **9a**–**d**.

Compd.	R^4	R^3	IC_{50}[a] (μM)
1a	H	Et	9.32 ± 0.42
1b	H	H	14.69 ± 1.16
9a	CH_3	Et	13.46 ± 1.95
9b	$CH_2CH(CH_3)_2$	Et	9.54 ± 1.99
9c	Ph	Et	8.44 ± 1.68
9d	Ph	H	10.89 ± 1.08

[a] Values are the mean ± SD (n = 3). Oleanolic acid was employed as a positive control (IC_{50} = 2.01 ± 0.26 μM).

Table 2
PTP1B inhibition data for compounds **14a**–**f**.

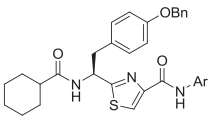

Compd.	Ar	IC_{50}[a] (μM)
14a	2-COOMe-Ph	8.79 ± 1.60
14b	3-COOMe-Ph	10.55 ± 1.48
14c	4-COOMe-Ph	4.42 ± 0.85
14d	2-COOH-Ph	8.12 ± 0.98
14e	3-COOH-Ph	6.00 ± 0.43
14f	4-COOH-Ph	4.88 ± 0.60

[a] Values are the mean ± SD (n = 3). Oleanolic acid was employed as a positive control (IC_{50} = 2.01 ± 0.26 μM).

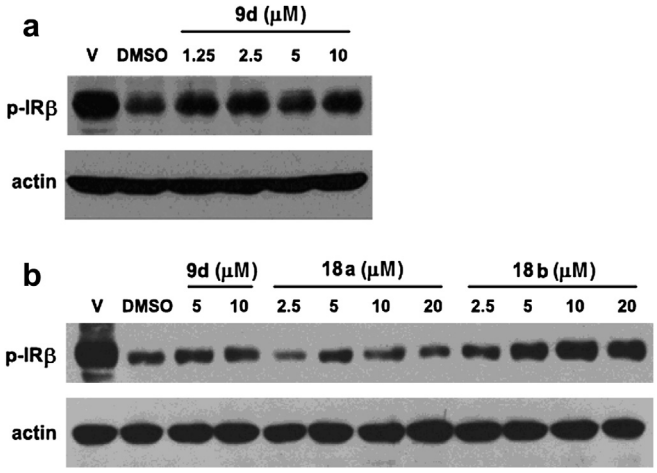

Fig. 2. Immunoblot analysis of PTP1B inhibitors in CHO-hIR cells. (a) Effect of **9d** on IRβ phosphorylation in CHO-hIR cells. (b) Effect of **18a** and **18b** on IRβ phosphorylation in CHO-hIR cells. CHO-hIR cells were incubated with 1 mM sodium orthovanadate (V), 0.2% DMSO, or compound **9d**, **18a**, or **18b** for 2 h, and then treated with 10 nM insulin for 10 min. Cell lysates were probed with anti-pTyr antibody. β-Actin was used as a loading control. V: 1 mM sodium orthovanadate used as a positive control.

signaling and glucose homeostasis [34]. Although it's proposed that the combined inhibition of PTP1B and TCPTP may prove useful in ameliorating glucose homeostasis and preventing obesity and diabetes [35], achieving pharmacological inhibition clinically at a corresponding level would be challenging and the clinical outcome of pharmacological inhibition of TCPTP continues to be debated. Hence, although challenging, selectivity over TCPTP remains a desirable profile for PTP1B inhibitors. To examine the selectivity profile of PTA derivatives, several representative compounds, **17b**, **18b**, **g**, **k** and **l**, were tested as inhibitors against a variety of different phosphatases, including TCPTP, CDC25B, SHP-1, SHP-2 and LAR. As shown in Table 5, the representative compounds showed modest selectivity (2.6- to 3.5-fold) over TCPTP, which has the highest homology to PTP1B, with 74% sequence identity in the catalytic domain. Compound **18g** showed 2.6-, 3.0- and 18.3-fold selectivity for PTP1B over TCPTP, CDC25B and SHP-2, respectively, and greater than 20-fold selectivity over SHP-1 and LAR.

3.3. Cellular activity

Given the observed inhibitory activity of compound **18g**, which emerged as the most potent inhibitor of PTP1B among all the analogs tested, we proceeded to evaluate its ability to inhibit PTP1B inside cells. As shown in Fig. 3a, incubation of CHO-hIR cells with **18g** in 5–20 μM concentration range increased insulin-mediated IRβ phosphorylation in a concentration-dependent manner. Metabolic insulin signal transduction occurs through insulin binding to its cell surface receptor (IR), upon which IR undergoes autophosphorylation on several tyrosine residues located in its activation loop [12]. Autophosphorylation increases IR kinase activity and leads to the recruitment of IRS proteins, which causes activation of phosphatidylinositol 3-kinase (PI3K) and downstream protein kinase B (Akt) [36]. The PI3K–Akt pathway is responsible for most of the metabolic action of insulin including the translocation of glucose transporter 4 (GLUT4) to the plasma membrane, which allows the uptake of extracellular glucose into skeletal muscle [37]. PTP1B inhibitors are thought to enhance the insulin-induced PI3K–Akt pathway [2]. We used western blot analysis to examine whether **18g** could augment the insulin-mediated PI3K–Akt pathway. Akt phosphorylation level was compared between untreated and **18g**-treated differentiated L6 myotubes. As shown in Figure 3b, **18g** treatment increased insulin-induced Akt phosphorylation. To investigate the role of compound **18g** in activating Akt, we treated L6 myotubes with wortmannin, a potent and selective PI3K inhibitor [38]. As shown in Fig. 3c, **18g**-stimulated insulin-dependent Akt phosphorylation in L6 myotubes was suppressed by 250 nM wortmannin, indicating that compound **18g** effectively inhibited intracellular PTP1B and subsequently activated the insulin-induced PI3K–Akt signaling pathways.

In insulin signaling pathway, a key action of insulin is the promotion of glucose uptake into cells by inducing the translocation of GLUT4 from intracellular storage to the plasma membrane. Previous studies have demonstrated that Akt mediates insulin-stimulated GLUT4 translocation and Akt activation should lead to increased glucose uptake [37]. To further evaluate the biological consequences of the increased IRβ and Akt phosphorylation levels stimulated by **18g**, we tested this compound in differentiated L6 myotubes to assess its ability to stimulate glucose uptake. As shown in Fig. 3d, L6 myotubes treated with **18g** displayed a concentration-

Table 3
PTP1B inhibition data for compounds **17a**, **b** and **18a**, **b**.

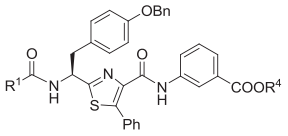

Compd.	R^1	R^4	IC_{50}[a] (μM)
17a	Cyclohexyl	Me	3.79 ± 0.67
17b	Cyclohexyl	H	1.17 ± 0.09
18a	2-(1*H*-Indol-3-yl)-ethyl	Me	2.68 ± 0.18
18b	2-(1*H*-Indol-3-yl)-ethyl	H	1.01 ± 0.07

[a] Values are the mean ± SD ($n = 3$). Oleanolic acid was employed as a positive control ($IC_{50} = 2.01 \pm 0.26$ μM).

Table 4
PTP1B inhibition data for compounds **18c**–**n**.

Compd.	Ar	IC_{50}[a] (μM)
18c	2-COOH-Ph	5.56 ± 0.68
18d	4-COOH-Ph	2.28 ± 0.67
18e	2-COOH-3F-Ph	4.18 ± 0.50
18f	2-COOH-4F-Ph	2.82 ± 0.72
18g	2-COOH-5F-Ph	0.54 ± 0.18
18h	2-COOH-5Cl-Ph	0.71 ± 0.11
18i	2-COOH-5Br-Ph	1.18 ± 0.21
18j	3-COOH-4F-Ph	1.62 ± 0.51
18k	3-COOH-4Cl-Ph	1.42 ± 0.41
18l	5-COOH-2F-Ph	1.12 ± 0.20
18m	4-COOH-2F-Ph	0.77 ± 0.12
18n	4-COOH-3F-Ph	2.56 ± 0.61

[a] Values are the mean ± SD ($n = 3$). Oleanolic acid was employed as a positive control ($IC_{50} = 2.01 \pm 0.26$ μM).

Table 5
Inhibition of PTPases by selected PTA derivatives.

	IC_{50} (μM)					
	PTP1B	TCPTP	CDC25B	SHP-1	SHP-2	LAR
17b	1.17 ± 0.09	3.97 ± 0.50	2.51 ± 0.02	6.93 ± 0.33	11.66 ± 0.91	>20
18b	1.01 ± 0.07	3.38 ± 0.42	7.37 ± 0.71	7.53 ± 0.74	5.30 ± 0.46	>20
18g	0.54 ± 0.18	1.42 ± 0.11	1.62 ± 0.11	12.64 ± 0.41	9.89 ± 2.18	>20
18k	1.42 ± 0.41	3.36 ± 0.46	4.94 ± 0.22	8.79 ± 0.32	6.79 ± 0.50	>20
18l	1.12 ± 0.20	3.98 ± 0.50	9.74 ± 0.81	10.61 ± 0.97	10.15 ± 0.97	>20

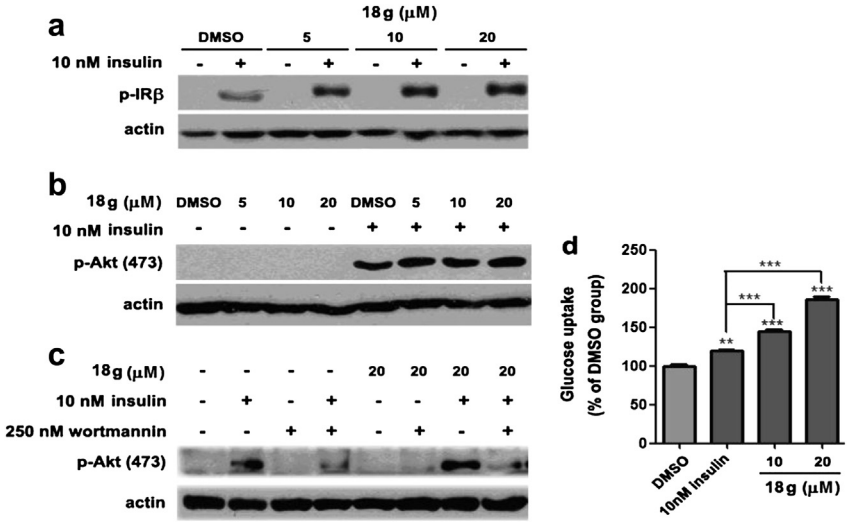

Fig. 3. Compound **18g** stimulates the insulin signaling pathway in cells. (a) Effect of **18g** on insulin-mediated IRβ phosphorylation in CHO-hIR cells. CHO-hIR cells were incubated with 0.2% DMSO or compound **18g** for 2 h and then incubated with or without 10 nM insulin for 10 min. Cell lysates were probed with anti-pTyr antibody. (b) Effect of **18g** on Akt phosphorylation in L6 myotubes. Differentiated L6 myotubes were incubated with 0.2% DMSO or compound **18g** for 2 h and then incubated with or without 10 nM insulin for 10 min. Cell lysates were immunoblotted with anti-phospho-Akt (Ser473) antibody. (c) The **18g**-stimulated phosphorylation of Akt is PI3K-dependent. L6 myotubes were pretreated with 250 nM wortmannin and then with 20 μM **18g** for 2 h, after which the cells were stimulated with or without 10 nM insulin for 30 min. Cell lysates were probed with anti-phospho-Akt (Ser473) antibody. β-Actin was used as a loading control. (d) Effect of **18g** on glucose uptake in L6 myotubes. L6 myotubes were serum starved for 2 h and then incubated with **18g** for 2 h followed by stimulation with 10 nM insulin for 30 min. The rate of glucose uptake was measured following the addition of 2-deoxy-[^{3}H]-deoxyglucose at 37 °C for 15 min. The graph shows the average of at least three independent replicates.

dependent increase in the rate of glucose uptake. The rate of glucose uptake was increased by 40% and 86% in the presence of 10 and 20 μM **18g**, respectively.

3.4. Molecular docking

The full-length PTP1B consists of 435 amino acids, of which residues 30–278 comprise the catalytic domain. The main structural features of PTP1B catalytic domain are the phosphate-binding loop, the WPD loop and the second aryl phosphate-binding site. The phosphate-binding loop (P-loop, His214–Arg221), which contains the catalytic residue Cys215, mediates the substrate recognition and binding of the phosphotyrosine deep in the catalytic site [39]. Upon substrate binding, the WPD loop (Thr177–Pro185) closes down onto the substrate and thereby positions the thiolate of Cys215 for the nucleophilic attack upon the phosphotyrosine [40,41]. The second aryl phosphate-binding site adjacent to the catalytic site is lined by Arg24, Asp48, Val49, Ile219, Arg254, Met258, Gly259 and Gln262 [42]. It's proposed that dual-binding inhibitors that occupy both the active site and second aryl phosphate-binding site would provide not only increased binding affinity but also the opportunity for improved selectivity over highly homologous phosphatase TCPTP [24,27,42,43]. To obtain structural information about the binding mode of inhibitors of PTP1B for further structural optimization, we used the LibDock protocol, available in Discovery Studio 2.1, to examine the molecular docking of compounds **18g** and **9d** into the active site of PTP1B in the open conformation. The X-ray crystal structure of PTP1B (PDB-ID: 1NNY) was retrieved from the RCSB Protein Data Bank (http://www.rcsb.org). As shown in Fig. 4a, compound **18g** bound both the catalytic site and the second aryl phosphate-binding site. Three hydrogen bonds were formed between the carboxylate group and the side chains of Gln266 and Arg221, and one hydrogen bond was formed between the fluorine atom and the side chain of Lys116. The indole side chain of compound **18g** fully occupied the second aryl phosphate-binding site and formed a cation–π interaction with the guanidine side chain of Arg24. By

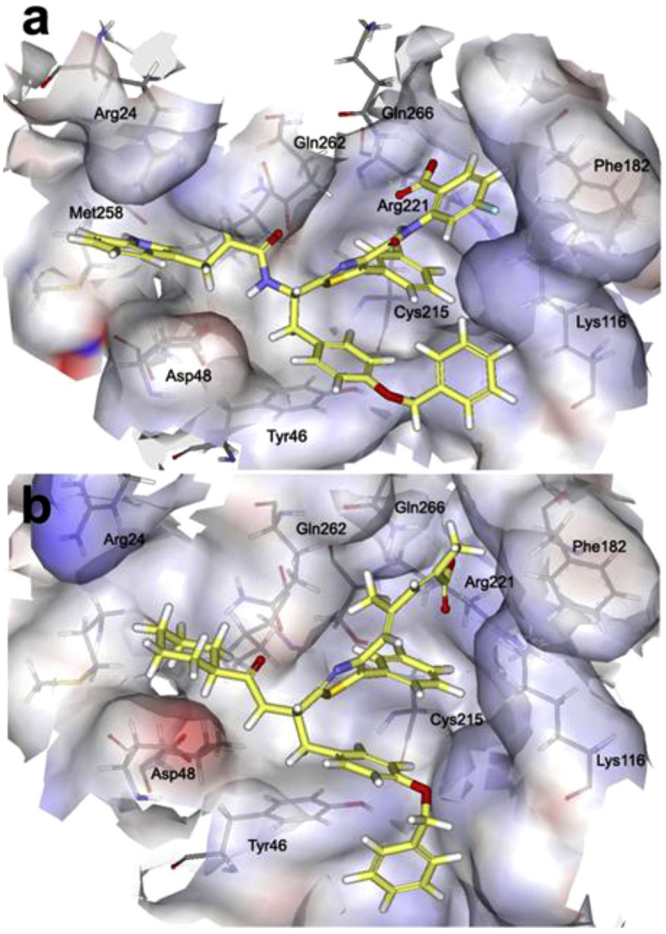

Fig. 4. Proposed binding modes of (a) **18g** and (b) **9d**. Ligands are shown in stick representation with carbon atoms in yellow. Hydrogen bonds are displayed as a green dashed line. The crystal structure of PTP1B, available from the RCSB Protein Data Bank (PDB: 1NNY), was used to examine the docking. (For interpretation of the references to color in this figure legend, the reader is referred to the web version of this article.)

contrast, compound **9d** did not fully occupy the second aryl phosphate-binding site (Fig. 4b). Four hydrogen bonds were formed between the carboxylate group of **9d** and the side chains of Gln266 and Arg221. These proposed binding modes show that compound **18g** positioned itself effectively in the PTP1B active site pocket and fully occupied both the catalytic site and the second aryl phosphate-binding site. This correlated well with the significantly improved inhibitory activity of **18g** compared with its ACT-derived analogs.

4. Conclusion

In this work, we identified and characterized a novel structural class of PTP1B inhibitors inspired from the key ACT scaffold of Scleritodermin A: the 2-ethyl-5-phenylthiazole-4-carboxamide (PTA) derivatives (as exemplified by compounds **18b** and **g**). Replacement of the conjugated diene moiety with the amide-linked aryl group provided a concise route for the synthesis of these PTP1B inhibitors. In the PTA skeleton, the phenyl group at the C5 position of the thiazole moiety contributed to the improved inhibitory activity of PTA derivatives compared with ACT or 2-ethylthiazole-4-carboxamide derivatives and improved their membrane permeability and cellular efficacy. In addition, the introduction of halogen atoms in the phenyl ring at site C further improved the inhibitory activity of PTA derivatives. The fluorinated analog **18g** displayed a submicromolar IC_{50} value against PTP1B and remarkable potency in cell-based assays. Compound **18g** dose dependently increased the insulin-induced phosphorylation of IRβ and Akt, the key molecules in the insulin signaling pathway, in the low micromolar range and effectively stimulated glucose uptake in L6 myotubes. Further improvements of compound **18g** and its structurally related analogs may lead to the development of a novel class of therapeutic agents for antidiabetes treatment.

5. Experimental section

5.1. Chemistry

5.1.1. General methods

Starting materials, reagents and solvents were purchased from commercial suppliers and used without further purification, unless otherwise stated. Anhydrous THF and CH_2Cl_2 were obtained from a distillation over sodium wire or CaH_2. All non-aqueous reactions were run under an inert atmosphere (nitrogen or argon) with rigid exclusion of moisture from reagents and all reaction vessels were oven-dried. The progress of reactions was monitored by silica gel thin layer chromatography (TLC) plates, visualized under UV or charred using phosphomolybdic acid solution followed by heating. Products were purified by flash column chromatography (FCC) on 200–300 mesh silica gel. Petroleum ether refers to the fraction with boiling range 60–90 °C or 30–60 °C. Proton nuclear magnetic resonance spectra (^{1}H NMR) were recorded on a spectrometer operating at 300 MHz. Data is reported as follows: chemical shift, multiplicity (s = singlet, d = doublet, dd = double doublet, t = triplet, q = quartet, br = broad, m = multiplet) and integration. Carbon nuclear magnetic resonance spectra (^{13}C NMR) were recorded on a spectrometer operating at 75 MHz. High-resolution mass data were obtained on a Micromass Q-Tof UltimaTM spectrometer. Purity was evaluated by analytical HPLC chromatograms using Agilent 1200 series LC system equipped with Zorbax SB C18 column, 4.6 × 150 mm, 5 μm particle size, at room temperature. Mobile phase: MeOH: 0.1% TFA in H_2O (80:20). Flow rate: 1.0 mL/min. UV detection: 285 nm.

5.1.2. (2Z,4E)-5-(2-((S)-2-(4-(Benzyloxy)phenyl)-1-(cyclohexanecarboxamido)ethyl) thiazol-4-yl)-2,4-dimethylpenta-2,4-dienoic acid (**1b**)

To a solution of **1a** (202 mg, 1.0 eq, 0.353 mmol) in dioxane/H_2O (2 mL/2 mL) was added LiOH···H_2O (148 mg, 10 eq, 3.53 mmol) and the solution was refluxed overnight. It was cooled and diluted with ethyl acetate and the water layer was acidified with 1 M HCl. The organic layer was then washed with water and brine, dried over Na_2SO_4 and concentrated in vacuo. The residue was purified by chromatography (CH_2Cl_2/MeOH = 7/1) to afford acid **1b** (192 mg, 100%). ^{1}H NMR (300 MHz, $CDCl_3$): δ 1.30–1.44 (m, 4H), 1.66–1.80 (m, 6H), 2.03 (s, 3H), 2.07 (m, 1H), 2.15 (s, 3H), 3.19 (br, 2H), 5.00 (s, 2H), 5.53 (d, 1H, *J* = 7.8 Hz), 6.36 (s, 1H), 6.58 (s, 1H), 6.84 (d, 2H, *J* = 8.4 Hz), 6.98 (d, 2H, *J* = 8.4 Hz), 7.01 (s, 1H), 7.30–7.42 (m, 5H). ^{13}C NMR (75 MHz, $CDCl_3$): δ 18.0, 21.8, 25.7, 29.4, 29.5, 40.6, 45.3, 51.9, 67.1, 70.0, 114.9, 117.0, 124.1, 127.6, 128.0, 128.6, 128.9, 129.3, 130.5, 136.9, 137.0, 138.5, 152.7, 157.7, 170.3, 173.6, 176.1. HRMS (ESI) *m*/*z* calc for $C_{32}H_{36}N_2O_4S$ $[M + H]^+$ is 545.2469, found 545.2466.

5.1.3. Ethyl2-((S)-3-(4-(benzyloxy)phenyl)-2-(tert-butoxycarbonylamino)propanamido)-3-oxo-3-phenylpropanoate (**2c**)

To a solution of Boc-L-Tyr(Bn)-OH (7.6 g, 1.0 eq, 20.5 mmol) in CH_2Cl_2 (100 mL) was added EDC hydrochloride (5.9 g, 1.5 eq, 30.8 mmol), DMAP (0.5 g, 0.2 eq, 4.1 mmol), Et_3N (5.9 mL, 2.0 eq, 41.0 mmol) and PhC(O)CH(NH_2)COOEt (5.0 g, 1.0 eq, 20.5 mmol). The reaction mixture was stirred at room temperature for 2 h. After the solvent was concentrated in vacuo, the residue was purified by chromatography (petroleum ether/ethyl acetate = 4/1) to afford **2c** as colorless gum (7.8 g, 68%). ^{1}H NMR (300 MHz, $CDCl_3$): δ 1.35 (t, 3H, *J* = 6.9 Hz), 1.41 (s, 9H), 2.98–3.09 (m, 2H), 4.14 (q, 2H, *J* = 6.9 Hz), 4.46 (m, 1H), 5.00 (s, 1H), 5.02 (s, 2H), 6.12 (d, 1H, *J* = 10.8 Hz), 6.84–6.89 (m, 4H), 7.09 (t, 2H, *J* = 8.4 Hz), 7.29–7.40 (m, 3H), 7.50 (t, 2H, *J* = 7.8 Hz), 7.64 (t, 1H, *J* = 7.8 Hz), 8.01 (t, 2H, *J* = 7.8 Hz).

5.1.4. (S)-Ethyl 2-(2-(4-(benzyloxy)phenyl)-1-(tert-butoxycarbonylamino)ethyl)-5-phenylthiazole-4-carboxylate (**3c**)

A solution of compound **2c** (509 mg, 1.0 eq, 0.91 mmol) and Lawesson's reagent (918 mg, 2.5 eq, 2.3 mmol) in dry THF (30 mL) was heated at 65 °C for 2 h. Then the reaction mixture was allowed to reach room temperature and concentrated in vacuo. The residue was purified by chromatography (petroleum ether/ethyl acetate = 6:1) to afford **3c** as white solid (418 mg, 82%). ^{1}H NMR (300 MHz, $CDCl_3$): δ 1.19 (t, 3H, *J* = 7.2 Hz), 1.40 (s, 9H), 3.29 (m, 2H), 4.28 (q, 2H, *J* = 7.2 Hz), 5.04 (s, 2H), 5.24 (br, 1H), 6.90 (d, 2H, *J* = 8.4 Hz), 7.08 (d, 2H, *J* = 8.4 Hz), 7.32–7.43 (m, 10H).

5.1.5. (S)-tert-Butyl 2-(4-(benzyloxy)phenyl)-1-(4-formyl-5-phenylthiazol-2-yl) ethylcarbamate (**5c**)

$LiAlH_4$ (30 mg, 1.0 eq, 0.75 mmol) was added in several portions to a solution of ester **3c** (419 mg, 1.0 eq, 0.75 mmol) in dry THF (15 mL) at 0 °C. The mixture reaction was stirred at room temperature for 2 h and then quenched with $Na_2SO_4 \cdot 10H_2O$. The mixture was extracted with ethyl acetate and the organic layers were dried over Na_2SO_4 and concentrated in vacuo to obtain alcohol **4c** (340 mg, 88%), which was used in the next step without further purification. A solution of alcohol **4c** (340 mg, 1.0 eq, 0.66 mmol) and IBX (222 mg, 1.2 eq, 7.9 mmol) in toluene/DMSO (5 mL/2 mL) was heated at 50 °C for 2 h. The white solid was removed by filtration and the filtrate was diluted with ethyl acetate and washed successively with water, saturated sodium bicarbonate and brine. The organic layers were dried over Na_2SO_4 and concentrated in vacuo to give aldehyde **5c** (289 mg, 85%). ^{1}H NMR (300 MHz, $CDCl_3$): δ 1.41 (s, 9H), 3.29 (m, 2H), 5.04 (s, 2H), 5.22 (br, 2H), 6.90 (d,

2H, J = 8.4 Hz), 7.07 (d, 2H, J = 8.4 Hz), 7.31–7.44 (m, 5H), 7.48 (s, 5H), 9.91 (s, 1H).

*5.1.6. (S,E)-Ethyl 3-(2-(2-(4-(benzyloxy)phenyl)-1-(tert-butoxycarbonylamino)ethyl)-5-phenylthiazol-4-yl)-2-methylacrylate (**6c**)*

$(EtO)_2P(O)CH(CH_3)CO_2Et$ (614 mg, 6.0 eq, 2.58 mmol) in dry THF (2 mL) was added to a suspension of NaH (189 mg, 11.0 eq, 4.73 mmol, 60% in mineral oil) in dry THF (8 mL) at 0 °C. The reaction mixture was stirred for 30 min at room temperature. Then aldehyde **5c** (221 mg, 1.0 eq, 0.43 mmol) in THF (5 mL) was added. The mixture was stirred at room temperature for 4 h. The reaction was quenched with saturated NH_4Cl and extracted with ethyl acetate. The organic layer was washed with brine, dried over Na_2SO_4 and concentrated in vacuo. The crude product was purified by chromatography (petroleum ether/ethyl acetate = 12:1) to give ester **6c** (224 mg, 87%). ^{1}H NMR (300 MHz, $CDCl_3$): δ 1.29 (t, 3H, J = 7.8 Hz), 1.42 (s, 9H), 2.36 (m, 3H), 3.28 (d, 2H, J = 6.9 Hz), 4.22 (q, 2H, J = 7.8 Hz), 5.03 (s, 2H), 5.20 (br, 2H), 6.88 (d, 2H, J = 9.0 Hz), 7.07 (d, 2H, J = 9.0 Hz), 7.33–7.43 (m, 9H), 7.55 (d, 1H, J = 2.7 Hz).

*5.1.7. (S,E)-tert-Butyl 2-(4-(benzyloxy)phenyl)-1-(4-(2-methyl-3-oxoprop-1-enyl)-5-phenylthiazol-2-yl) ethylcarbamate (**7c**)*

Compound **7c** was prepared using similar procedures as for **5c**. Yield 80% for 2 steps from **6c**. ^{1}H NMR (300 MHz, $CDCl_3$): δ 1.42 (s, 9H), 2.30 (s, 3H), 3.30 (m, 2H), 5.02 (s, 2H), 5.23 (br, 2H), 6.89 (d, 2H, J = 8.4 Hz), 7.09 (d, 2H, J = 8.4 Hz), 7.11 (s, 1H), 7.32–7.46 (m, 10H), 9.49 (s, 1H).

*5.1.8. (2Z,4E)-Ethyl 5-(2-((S)-2-(4-(benzyloxy)phenyl)-1-(tert-butoxycarbonylamino) ethyl)-5-phenylthiazol-4-yl)-2,4-dimethylpenta-2,4-dienoate (**8c**)*

To a solution of $(CF_3CH_2O)_2P(O)CH(CH)_3CO_2Et$ (197 mg, 3.0 eq, 0.53 mmol) and 18-crown-6 (713 mg, 15.0 eq, 2.70 mmol) in THF at −78 °C was added KHMDS (1.06 mL, 3.0 eq, 0.5 mmol/mL, 0.53 mmol) and the reaction mixture was stirred for 1 h at −78 °C. Then aldehyde **7c** (99 mg, 1.0 eq, 0.18 mmol) was added and the mixture was stirred at −78 °C for 2 h. The reaction was quenched with saturated NH_4Cl and extracted with ethyl acetate. The organic layer was washed with brine, dried over Na_2SO_4 and concentrated in vacuo. The residue was purified by chromatography (petroleum ether/acetone = 15:1) to give ester **8c** (115 mg, 39%). ^{1}H NMR (300 MHz, $CDCl_3$): δ 1.26 (t, 3H, J = 7.8 Hz), 1.60 (s, 9H), 2.00 (s, 3H), 2.18 (s, 3H), 3.27 (m, 2H), 4.17 (q, 2H, J = 7.8 Hz), 5.03 (s, 2H), 5.21 (br, 2H), 6.20 (s, 1H), 6.33 (s, 1H), 6.88 (d, 2H, J = 8.4 Hz), 7.05 (t, 2H, J = 8.4 Hz), 7.31–7.43 (m, 10H).

*5.1.9. (2Z,4E)-Ethyl 5-(2-((S)-2-(4-(benzyloxy)phenyl)-1-(cyclohexanecarboxamido) ethyl)-5-phenylthiazol-4-yl)-2,4-dimethylpenta-2,4-dienoate (**9c**)*

To a solution of **8c** (30 mg, 1.0 eq, 0.047 mmol) in CH_2Cl_2 (2 mL), trifluoroacetic acid (0.4 mL) was added and the mixture was stirred for 2 h at room temperature. The reaction mixture evaporated in vacuo to afford the crude amine, which was used without further purification. A solution of the amine and DIPEA (0.1 mL, 10 eq, 0.47 mmol) in dry CH_2Cl_2 (5 mL) was cooled in an ice bath and then cyclohexanecarbonyl chloride (11 μL, 1.5 eq, 0.070 mmol) was added. The reaction mixture was stirred at room temperature overnight. After the solvent was concentrated in vacuo, the residue was purified by chromatography (petroleum ether/acetone = 9/1) to afford **9c** (21 mg, 69%). M.p. 130–132 °C. ^{1}H NMR (300 MHz, $CDCl_3$): δ 1.25 (t, 3H, J = 7.8 Hz), 1.28–1.45 (m, 4H), 1.68–1.88 (m, 6H), 2.00 (s, 3H), 2.09 (m, 1H), 2.17 (s, 3H), 3.27 (m, 2H), 4.17 (q, 2H, J = 7.8 Hz), 5.03 (s, 2H), 5.55 (q, 1H, J = 8.1 Hz), 6.20 (s, 1H), 6.30 (d, 1H, J = 8.1 Hz), 6.33 (s, 1H), 6.87 (d, 2H, J = 8.4 Hz), 7.05 (d, 2H, J = 8.4 Hz), 7.31–7.43 (m, 10H). ^{13}C NMR (75 MHz, $CDCl_3$): δ 14.2, 17.2, 22.1, 25.8, 29.7, 29.8, 40.6, 45.5, 52.2, 60.9, 70.2, 100.1, 115.0, 123.2, 127.7, 128.1, 128.3, 128.7, 128.9, 129.8, 130.8, 131.9, 137.3, 137.6, 157.9, 167.6, 170.6, 175.5. HRMS (ESI) m/z calc for $C_{40}H_{44}N_2O_4S$ $[M + H]^+$ is 649.3095, found 649.3092.

*5.1.10. (2Z,4E)-5-(2-((S)-2-(4-(Benzyloxy)phenyl)-1-(cyclohexanecarboxamido) ethyl)-5-phenylthiazol-4-yl)-2,4-dimethylpenta-2,4-dienoic acid (**9d**)*

Compound **9d** was prepared using similar procedures as for **1b**. Yield 90% from **9c**. M.p. 103–106 °C. ^{1}H NMR (300 MHz, $CDCl_3$): δ 1.10–1.42 (m, 7H), 1.68–1.88 (m, 6H), 2.05 (s, 3H), 2.09 (m, 1H), 2.17 (s, 3H), 3.24 (d, 2H, J = 7.8 Hz), 5.00 (s, 2H), 5.54 (q, 1H, J = 8.4 Hz), 6.30 (s, 1H), 6.36 (br, 1H), 6.86 (d, 2H, J = 7.8 Hz), 6.90 (m, 1H), 7.06 (d, 2H, J = 8.4 Hz), 7.30–7.39 (m, 9H). ^{13}C NMR (75 MHz, $CDCl_3$): δ 17.6, 23.0, 26.1, 26.2, 40.4, 45.5, 52.4, 52.6, 70.5, 115.3, 121.7, 128.1, 128.5, 128.6, 129.1, 129.2, 129.8, 130.2, 131.0, 131.1, 132.3, 135.5, 137.6, 140.2, 148.1, 158.2, 169.4, 176.7. HRMS (ESI) m/z calc for $C_{38}H_{40}N_2O_4S$ $[M + H]^+$ is 621.2782, found 621.2780.

*5.1.11. Compounds **2a**–**9a**, **2b**–**9b** were prepared using similar procedures as for **2c**–**9c***

*5.1.11.1. Ethyl 2-((S)-3-(4-(benzyloxy)phenyl)-2-(tert-butoxycarbonylamino) propanamido)-3-oxobutanoate (**2a**).* Yield 47% from Boc-L-Tyr(Bn)-OH. ^{1}H NMR (300 MHz, $CDCl_3$): δ 1.29 (td, 3H, J = 2.1, 7.8 Hz), 1.40 (s, 9H), 2.35 (s, 3H), 3.04 (m, 2H), 4.25 (dq, 2H, J = 2.1, 7.8 Hz), 4.42 (br, 1H), 5.02 (s, 2H), 5.19 (dd, 1H, J = 2.1, 7.8 Hz), 6.90 (d, 2H, J = 8.1 Hz), 7.12 (d, 2H, J = 8.1 Hz), 7.31–7.43 (m, 5H).

*5.1.11.2. Ethyl 2-((S)-3-(4-(benzyloxy)phenyl)-2-(tert-butoxycarbonylamino) propanamido)-5-methyl-3-oxohexanoate (**2b**).* Yield 60% from Boc-L-Tyr(Bn)-OH. ^{1}H NMR (300 MHz, $CDCl_3$): δ 0.90 (dd, 6H, J = 6.3, 13.2 Hz), 1.26 (t, 3H, J = 7.8 Hz), 1.39 (s, 9H), 2.17 (m, 1H), 2.55 (t, 2H, J = 7.8 Hz), 3.04 (m, 2H), 4.22 (m, 2H), 4.42 (m, 1H), 5.00 (s, 2H), 5.16 (br, 2H), 6.88 (d, 2H, J = 8.4 Hz), 7.11 (d, 2H, J = 8.4 Hz), 7.28–7.41 (m, 5H).

*5.1.11.3. (S)-Ethyl 2-(2-(4-(benzyloxy)phenyl)-1-(tert-butoxycarbonylamino)ethyl)-5-methylthiazole-4-carboxylate (**3a**).* Yield 76% from **2a**. ^{1}H NMR (300 MHz, $CDCl_3$): δ 1.25–1.43 (m, 12H), 2.69 (s, 3H), 3.22 (m, 2H), 4.21 (q, 2H, J = 7.8 Hz), 5.02 (s, 2H), 5.19 (m, 2H), 6.87 (d, 2H, J = 8.4 Hz), 7.03 (d, 2H, J = 8.4 Hz), 7.30–7.42 (m, 5H).

*5.1.11.4. (S)-Ethyl 2-(2-(4-(benzyloxy)phenyl)-1-(tert-butoxycarbonylamino)ethyl)-5-isobutylthiazole-4-carboxylate (**3b**).* Yield 81% from **2b**. ^{1}H NMR (300 MHz, $CDCl_3$): δ 0.90 (dd, 6H, J = 6.6, 13.8 Hz), 1.26 (t, 3H, J = 7.8 Hz), 1.39 (s, 9H), 2.17 (m, 1H), 2.55 (t, 2H, J = 7.8 Hz), 3.04 (m, 2H), 4.22 (q, 2H, J = 7.8 Hz), 4.44 (m, 1H), 5.00 (s, 2H), 5.16 (br, 2H), 6.88 (d, 2H, J = 8.4 Hz), 7.11 (d, 2H, J = 8.4 Hz), 7.28–7.41 (m, 5H).

*5.1.11.5. (S)-tert-Butyl 2-(4-(benzyloxy)phenyl)-1-(4-formyl-5-methylthiazol-2-yl) ethylcarbamate (**5a**).* Yield 81% for 2 steps from **3a**. ^{1}H NMR (300 MHz, $CDCl_3$): δ 1.41 (s, 9H), 2.73 (s, 3H), 3.22 (d, 2H, J = 6.6 Hz), 5.03 (s, 2H), 6.88 (d, 2H, J = 7.8 Hz), 7.03 (d, 2H, J = 7.8 Hz), 7.35–7.41 (m, 5H), 10.11 (s, 1H).

*5.1.11.6. (S)-tert-Butyl 2-(4-(benzyloxy)phenyl)-1-(4-formyl-5-isobutylthiazol-2-yl) ethylcarbamate (**5b**).* Yield 91% for 2 steps from **3b**. ^{1}H NMR (300 MHz, $CDCl_3$): δ 0.94 (d, 6H, J = 6.9 Hz), 1.41 (s, 9H), 1.88 (m, 1H), 3.06 (d, 2H, 7.8 Hz), 3.21 (d, 2H, J = 6.9 Hz), 5.02 (s, 2H), 5.20 (m, 2H), 6.87 (d, 2H, J = 9.0 Hz), 7.10 (d, 2H, J = 9.0 Hz), 7.31–7.43 (m, 5H), 10.09 (s, 1H).

*5.1.11.7. (S,E)-Ethyl 3-(2-(2-(4-(benzyloxy)phenyl)-1-(tert-butoxycarbonylamino) ethyl)-5-methylthiazol-4-yl)-2-methylacrylate (**6a**).*

Yield 73% from **5a**. ^{1}H NMR (300 MHz, $CDCl_3$): δ 1.35 (t, 3H, J = 7.8 Hz), 1.55 (s, 9H), 2.34 (d, 3H, J = 2.7 Hz), 2.45 (s, 3H), 3.22 (d, 2H, J = 6.9 Hz), 4.27 (q, 2H, J = 7.8 Hz), 5.03 (s, 2H), 5.13 (br 2H), 6.86 (d, 2H, J = 9.0 Hz), 7.02 (d, 2H, J = 9.0 Hz), 7.31–7.43 (m, 4H), 9.50 (d, 1H, J = 2.7 Hz).

*5.1.11.8. (S,E)-Ethyl 3-(2-(2-(4-(benzyloxy)phenyl)-1-(tert-butoxycarbonylamino) ethyl)-5-isobutylthiazol-4-yl)-2-methylacrylate (**6b**).* Yield 75% from **5b**. ^{1}H NMR (300 MHz, $CDCl_3$): δ 0.92 (d, 6H, J = 7.8 Hz), 1.34 (t, 3H, J = 7.8 Hz), 1.42 (s, 9H), 1.81 (m, 1H), 2.35 (d, 3H, J = 2.1 Hz), 2.69 (d, 2H, J = 7.8 Hz), 3.21 (br 2H), 4.27 (q, 2H, J = 7.8 Hz), 5.02 (s, 2H), 5.16 (br, 2H), 6.85 (d, 2H, J = 8.4 Hz), 7.00 (d, 2H, J = 8.4 Hz), 7.31–7.43 (m, 4H), 7.51 (d, 1H, J = 2.1 Hz).

*5.1.11.9. (S,E)-tert-Butyl 2-(4-(benzyloxy)phenyl)-1-(5-methyl-4-(2-methyl-3-oxoprop-1-enyl)thiazol-2-yl)ethylcarbamate (**7a**).* Yield 80% for 2 steps from **6a**. ^{1}H NMR (300 MHz, $CDCl_3$): δ 1.42 (s, 9H), 2.27 (s, 3H), 2.53 (s, 3H), 3.23 (d, 2H, J = 6.6 Hz), 5.03 (s, 2H), 5.14 (m, 2H), 6.87 (d, 2H, J = 8.4 Hz), 7.03 (d, 2H, J = 8.4 Hz), 7.06 (s, 1H), 7.30–7.43 (m, 5H), 9.60 (s, 1H).

*5.1.11.10. (S,E)-tert-Butyl 2-(4-(benzyloxy)phenyl)-1-(5-isobutyl-4-(2-methyl-3-oxoprop-1-enyl)thiazol-2-yl)ethylcarbamate (**7b**).* Yield 60% for 2 steps from **6b**. ^{1}H NMR (300 MHz, $CDCl_3$): δ 0.95 (d, 6H, J = 7.8 Hz), 1.42 (s, 9H), 1.86 (m, 1H), 2.28 (s, 3H), 2.76 (d, 2H, J = 7.8 Hz), 3.23 (d, 2H, J = 6.6 Hz), 5.02 (s, 2H), 5.16 (br, 2H), 6.86 (d, 2H, J = 8.4 Hz), 7.00 (s, 1H), 7.04 (d, 2H, J = 8.4 Hz), 7.31–7.43 (m, 5H), 9.60 (s, 1H).

*5.1.11.11. (2Z,4E)-Ethyl 5-(2-((S)-2-(4-(benzyloxy)phenyl)-1-(tert-butoxycarbonylamino)ethyl)-5-methylthiazol-4-yl)-2,4-dimethylpenta-2,4-dienoate (**8a**).* Yield 67% from **7a**. ^{1}H NMR (300 MHz, $CDCl_3$): δ 1.30 (t, 3H, J = 7.8 Hz), 1.41 (s, 9H), 2.03 (s, 3H), 2.14 (s, 3H), 2.32 (s, 3H), 3.20 (d, 2H, J = 6.6 Hz), 4.20 (q, 2H, J = 7.8 Hz), 5.02 (s, 2H), 5.16 (br, 2H), 6.27 (br, 2H), 6.85 (d, 2H, J = 9.0 Hz), 7.02 (d, 2H, J = 9.0 Hz), 7.31–7.43 (m, 5H).

*5.1.11.12. (2Z,4E)-Ethyl 5-(2-((S)-2-(4-(benzyloxy)phenyl)-1-(tert-butoxycarbonylamino)ethyl)-5-isobutylthiazol-4-yl)-2,4-dimethylpenta-2,4-dienoate (**8b**).* Yield 36% from **7b**. ^{1}H NMR (300 MHz, $CDCl_3$): δ 0.90 (d, 6H, J = 6.6 Hz), 1.28 (t, 3H, J = 7.8 Hz), 1.42 (s, 9H), 1.87 (m, 1H), 2.03 (s, 3H), 2.17 (s, 3H), 2.58 (d, 2H, J = 7.8 Hz), 3.21 (d, 2H, J = 6.6 Hz), 4.20 (q, 2H, J = 7.8 Hz), 5.01 (s, 2H), 5.18 (br, 2H), 6.26 (br, 2H), 6.84 (d, 2H, J = 9.0 Hz), 6.95 (d, 2H, J = 8.7 Hz), 7.31–7.43 (m, 5H).

*5.1.11.13. (2Z,4E)-Ethyl 5-(2-((S)-2-(4-(benzyloxy)phenyl)-1-(cyclohexanecarboxamido)ethyl)-5-methylthiazol-4-yl)-2,4-dimethylpenta-2,4-dienoate (**9a**).* Yield 36% for 2 steps from **8a**. ^{1}H NMR (300 MHz, $CDCl_3$): δ 1.27 (t, 3H, J = 7.9 Hz), 1.29–1.43 (m, 4H), 1.66–1.86 (m, 6H), 2.03 (s, 3H), 2.07 (m, 1H), 2.11 (s, 1H), 2.32 (s, 3H), 3.20 (d, 2H, J = 6.6 Hz), 4.20 (q, 2H, J = 7.2 Hz), 5.02 (s, 2H), 5.45 (q, 1H, J = 8.4 Hz), 6.26 (br, 2H), 6.31 (d, 1H, J = 8.4 Hz), 6.84 (d, 2H, J = 9.0 Hz), 6.99 (d, 2H, J = 9.0 Hz), 7.31–7.43 (m, 5H). ^{13}C NMR (75 MHz, $CDCl_3$): δ 11.8, 14.2, 17.1, 21.9, 25.8, 29.6, 29.7, 40.6, 45.5, 52.0, 60.9, 70.1, 114.9, 122.0, 127.6, 128.1, 128.7, 129.0, 129.1, 130.7, 131.1, 136.4, 137.2, 137.6, 148.6, 157.8, 165.8, 175.5. HRMS (ESI) m/z calc for $C_{35}H_{42}N_2O_4S$ $[M + H]^+$ is 587.2938, found 587.2934.

*5.1.11.14. (2Z,4E)-Ethyl 5-(2-((S)-2-(4-(benzyloxy)phenyl)-1-(cyclohexanecarboxamido)ethyl)-5-isobutylthiazol-4-yl)-2,4-dimethylpenta-2,4-dienoate (**9b**).* Yield 36% for 2 steps from **8b**. ^{1}H NMR (300 MHz, $CDCl_3$): δ 0.89 (dd, 6H, J = 2.1, 7.8 Hz), 1.26 (t, 3H, J = 7.8 Hz), 1.29–1.44 (m, 4H), 1.66–1.85 (m, 6H), 2.03 (s, 3H), 2.08 (m, 1H), 2.13 (s, 3H), 2.56 (d, 2H, J = 7.8 Hz), 3.20 (dd, 2H, J = 2.7, 7.8 Hz), 4.20 (q, 2H, J = 7.8 Hz), 5.01 (s, 2H), 5.47 (q, 1H, J = 7.8 Hz), 6.25 (br, 2H), 6.36 (d, 1H, J = 8.4 Hz), 6.82 (d, 2H, J = 8.4 Hz), 6.96 (d, 2H, J = 8.4 Hz), 7.31–7.42 (m, 5H). ^{13}C NMR (75 MHz, $CDCl_3$): δ 14.3, 17.1, 22.0, 22.3, 25.6, 25.8, 25.9, 25.9, 29.1, 29.6, 29.7, 31.2, 35.5, 40.8, 45.5, 52.1, 60.8, 70.1, 114.8, 122.2, 127.6, 128.1, 128.7, 129.0, 130.7, 136.2, 136.3, 137.2, 137.7, 148.6, 157.8, 160.8, 165.9, 169.8, 170.6, 175.5. HRMS (ESI) m/z calc for $C_{38}H_{48}N_2O_4S$ $[M + H]^+$ is 629.3408, found 629.3420.

*5.1.12. Compound **10***

Compound **10** was synthesized as previously reported [44].

*5.1.13. (S)-Ethyl 2-(2-(4-(benzyloxy)phenyl)-1-(cyclohexanecarboxamido)ethyl) thiazole-4-carboxylate (**12**)*

Compound **12** was prepared using similar procedures from **10** as for **9c**. Yield 86% for 2 steps from **10**. ^{1}H NMR (300 MHz, $CDCl_3$): δ 1.41 (t, 3H, J = 7.2 Hz), 1.44–1.77 (m, 5H), 2.05–2.12 (m, 1H), 3.19–3.33 (m, 2H), 4.43 (q, 2H, J = 6.9 Hz), 5.02 (s, 2H), 5.55 (q, 1H, J = 8.1 Hz), 6.24 (d, 1H, J = 7.8 Hz), 6.86 (d, 2H, J = 8.4 Hz), 6.99 (d, 2H, J = 8.4 Hz), 7.27–7.43 (m, 5H), 8.02 (s, 1H).

*5.1.14. (S)-2-(2-(4-(Benzyloxy)phenyl)-1-(cyclohexanecarboxamido)ethyl)thiazole-4-carboxylic acid (**13**)*

Yield 99% from **12**. ^{1}H NMR (300 MHz, $CDCl_3$): δ 1.25–1.35 (m, 10H), 1.75–1.78 (m, 1H), 3.26 (d, 1H), 5.03 (s, 2H), 5.56 (q, 1H, J = 8.1 Hz), 6.11 (d, 1H, J = 8.4 Hz), 6.88 (d, 2H, J = 9.0 Hz), 6.99 (d, 1H, J = 8.7 Hz), 7.27–7.40 (m, 5H), 8.15 (s, 1H).

*5.1.15. General procedure for the synthesis of **14a–c***

To a solution **13** (30 mg, 1.0 eq, 0.065 mmol) in CH_2Cl_2 (100 mL) was added EDC hydrochloride (15 mg, 1.2 eq, 0.078 mmol), DMAP (2 mg, 0.2 eq, 0.013 mmol), Et_3N (20 μL, 2.0 eq, 0.156 mmol) and $HCl\cdot H_2NC_6H_4COOMe$ (15 mg, 1.2 eq, 0.078 mmol). The reaction mixture was stirred at room temperature overnight. After the solvent was concentrated in vacuo, the residue was purified by chromatography (petroleum ether/ethyl acetate = 4/1) to afford **14a–c**.

*5.1.15.1. (S)-Methyl 2-(2-(2-(4-(benzyloxy)phenyl)-1-(cyclohexanecarboxamido)ethyl) thiazole-4-carboxamido)benzoate (**14a**).* Yield 47%. M.p. 214–217 °C. ^{1}H NMR (300 MHz, $CDCl_3$): δ 1.48–1.93 (m, 10H), 2.04–2.08 (m, 1H), 3.09 (t, 1H, J = 6.3 Hz), 3.20–3.46 (m, 1H), 3.97 (s, 3H), 5.02 (d, 2H, J = 7.8 Hz), 5.61 (q, 1H, J = 6.3 Hz), 5.88 (d, 1H), 6.68 (d, 1H, J = 7.2 Hz), 6.85–7.06 (m, 5H), 7.15 (t, 1H, J = 6.3 Hz), 7.35–7.39 (m, 5H), 7.61 (t, 1H, J = 8.4 Hz), 8.10 (d, 1H, J = 7.5 Hz), 8.91 (d, 1H, J = 8.4 Hz). HRMS (ESI) m/z calc for $C_{34}H_{35}N_3O_5S$ $[M + H]^+$ is 598.2370, found 598.2368.

*5.1.15.2. (S)-Methyl 3-(2-(2-(4-(benzyloxy)phenyl)-1-(cyclohexane carboxamido)ethyl) thiazole-4-carboxamido)benzoate (**14b**).* Yield 73%. M.p. 130–131 °C. ^{1}H NMR (300 MHz, $CDCl_3$): δ 1.32–1.46 (m, 6H), 1.68–1.86 (m, 4H), 2.09–2.19 (m, 1H), 3.28 (d, 2H, J = 6.6 Hz), 3.89 (s, 3H), 5.02 (s, 2H), 5.60 (q, 2H, J = 8.1 Hz), 6.07 (d, 1H, J = 8.1 Hz), 6.89 (d, 2H, J = 8.4 Hz), 7.01 (d, 2H, J = 8.4 Hz), 7.31–7.49 (m, 7H), 7.83 (d, 1H, J = 7.8 Hz), 8.09 (s, 1H), 8.14 (d, 1H, J = 9.0 Hz), 8.19 (s, 1H), 9.22 (s, 1H). HRMS (ESI) m/z calc for $C_{34}H_{35}N_3O_5S$ $[M + H]^+$ is 598.2370, found 598.2370.

*5.1.15.3. (S)-Methyl 4-(2-(2-(4-(benzyloxy)phenyl)-1-(cyclohexan ecarboxamido)ethyl) thiazole-4-carboxamido)benzoate (**14c**).* Yield 61%. M.p. 148–151 °C. ^{1}H NMR (300 MHz, $CDCl_3$): δ 1.38–1.81 (m, 10H), 2.13–2.20 (m, 1H), 3.28 (d, 2H), 3.91 (s, 3H), 5.02 (s, 2H), 5.60 (m, 1H), 6.04 (d, 1H), 6.89 (d, 2H, J = 7.8 Hz), 7.00 (d, 2H, J = 7.8 Hz), 7.32–7.53 (m, 5H), 7.80 (d, 2H, J = 8.4 Hz), 8.06 (d, 2H, J = 8.7 Hz), 8.11 (s, 1H), 9.27 (s, 1H). HRMS (ESI) m/z calc for $C_{34}H_{35}N_3O_5S$ $[M + Na]^+$ is 620.2190, found 620.2190.

*5.1.16. General procedure for the synthesis of **14d–f***

To a solution of **14a–c** (20 mg, 1.0 eq, 0.033 mmol) in dioxane/H_2O (0.5 mL/0.5 mL) was added $LiOH\cdots H_2O$ (12 mg, 10 eq, 0.33 mmol) and the solution was stirred overnight at room temperature. It was diluted with ethyl acetate and the water layer was acidified with 1 M HCl. The organic layer was then washed with water and brine, dried over Na_2SO_4 and concentrated in vacuo. The residue was purified by chromatography (CH_2Cl_2/MeOH = 7/1) to afford acid **14d–f**.

*5.1.16.1. (S)-2-(2-(2-(4-(Benzyloxy)phenyl)-1-(cyclohexanecarboxamido)ethyl) thiazole-4-carboxamido)benzoic acid (**14d**).* Yield 98%. M.p. >240 °C. ^{1}H NMR (300 MHz, DMSO-d_6): δ 1.47–1.66 (m, 10H), 2.08–2.20 (m, 1H), 2.99–3.59 (m, 2H), 5.02 (s, 2H), 5.28 (m, 1H), 6.92 (d, 2H, J = 8.1 Hz), 7.10 (t, 2H), 7.24 (d, 2H, J = 8.1 Hz), 7.29–7.48 (m, 5H), 8.06 (d, 1H, J = 8.4 Hz), 8.31 (s, 1H), 8.59 (d, 1H, J = 8.1 Hz), 8.75 (d, 1H, J = 8.1 Hz). HRMS (ESI) m/z calc for $C_{33}H_{33}N_3O_5S$ $[M + Na]^+$ is 606.2033, found 606.2031.

*5.1.16.2. (S)-3-(2-(2-(4-(Benzyloxy)phenyl)-1-(cyclohexanecarboxamido)ethyl) thiazole-4-carboxamido)benzoic acid (**14e**).* Yield 98%. M.p. 201–203 °C. ^{1}H NMR (300 MHz, DMSO-d_6): δ 1.48–1.71 (m, 10H), 2.14 (m, 1H), 3.05 (t, 2H), 5.07 (s, 2H), 5.31 (m, 1H), 6.94 (d, 2H, J = 6.6 Hz), 7.23 (d, 2H, J = 6.6 Hz), 7.32–7.52 (m, 7H), 7.70 (d, 1H, J = 7.2 Hz), 8.08 (d, 1H, J = 8.1 Hz), 8.36 (s, 1H), 8.47 (s, 1H), 8.61 (d, 1H, J = 7.5 Hz), 10.33 (s, 1H). HRMS (ESI) m/z calc for $C_{33}H_{33}N_3O_5S$ $[M + Na]^+$ is 606.2033, found 606.2033.

*5.1.16.3. (S)-4-(2-(2-(4-(Benzyloxy)phenyl)-1-(cyclohexanecarboxamido)ethyl) thiazole-4-carboxamido)benzoic acid (**14f**).* Yield 92%. M.p. 173–176 °C. ^{1}H NMR (300 MHz, CD_3OD): δ 1.32–1.68 (m, 10H), 2.06–2.14 (m, 1H), 2.97–3.05 (m, 2H), 5.07 (s, 2H), 5.29 (m, 1H), 6.94 (d, 2H, J = 8.7 Hz), 7.22 (d, 2H, J = 8.4 Hz), 7.31–7.45 (m, 5H), 7.93–8.00 (m, 4H), 8.39 (s, 1H), 8.61 (d, 1H, J = 8.4 Hz), 10.37 (s, 1H). HRMS (ESI) m/z calc for $C_{33}H_{33}N_3O_5S$ $[M + Na]^+$ is 606.2033, found 606.2029.

*5.1.17. (S)-2-(2-(4-(Benzyloxy)phenyl)-1-(tert-butoxycarbonylamino)ethyl)-5-phenylthiazole-4-carboxylic acid (**15**)*

To a solution of **3c** (508 mg, 1.0 eq, 0.91 mmol) in THF/H_2O (10 mL/10 mL) was added $LiOH\cdots H_2O$ (230 mg, 6 eq, 6.0 mmol) and the solution was stirred overnight at 50 °C. It was cooled and diluted with ethyl acetate and the water layer was acidified with 1 M HCl. The organic layer was then washed with water and brine, dried over Na_2SO_4 and concentrated in vacuo to afford acid **15** (483 mg, 100%). ^{1}H NMR (300 MHz, $CDCl_3$): δ 1.40 (s, 9H), 3.21 (m, 2H), 5.00 (s, 2H), 5.14 (m, 1H), 6.87 (d, 2H, J = 8.4 Hz), 7.04 (d, 2H, J = 8.7 Hz), 7.28–7.46 (m, 10H).

*5.1.18. (S)-Methyl 3-(2-(2-(4-(benzyloxy)phenyl)-1-(tert-butoxycarbonylamino)ethyl)-5-phenylthiazole-4-carboxamido) benzoate (**16**)*

To a solution **15** (490 mg, 1.0 eq, 0.92 mmol) in CH_2Cl_2 (50 mL) was added HATU (525 mg, 1.5 eq, 1.38 mmol), 4-methylmorpholine (0.30 mL, 3.0 eq, 2.8 mmol) and methyl 3-aminobenzoate hydrochloride (208 mg, 1.2 eq, 1.1 mmol). The reaction mixture was stirred at room temperature overnight. After the solvent was concentrated in vacuo, the residue was purified by chromatography (petroleum ether/acetone = 3/1) to afford compound **16** as white solid (360 mg, 59%). ^{1}H NMR (300 MHz, $CDCl_3$): δ 1.44 (s, 9H), 3.28 (m, 2H), 3.91 (s, 3H), 5.04 (s, 2H), 5.15 (m, 1H), 6.93 (d, 2H, J = 8.7 Hz), 7.10 (d, 2H, J = 8.7 Hz), 7.31–7.46 (m, 8H), 7.54–7.57 (m, 2H), 7.75 (d, 1H, J = 8.4 Hz), 8.06 (d, 1H, J = 8.4 Hz), 8.14 (s, 1H), 9.43 (s, 1H).

*5.1.19. (S)-Methyl 3-(2-(2-(4-(benzyloxy)phenyl)-1-(cyclohexanecarboxamido)ethyl)-5-phenylthiazole-4-carboxamido) benzoate (**17a**)*

Compound **16** (131 mg, 0.20 mmol) was dissolved in 10 mL 4 M HCl/EtOAc. The solution was stirred overnight at room temperature. Then it was evaporated in vacuo to obtain the crude amine which was used in the next step without further purification. A solution of the crude amine (67 mg, 1.0 eq, 0.12 mmol) and Et_3N (38 μL, 2.2 eq, 0.26 mmol) in dry CH_2Cl_2 (5 mL) was cooled in an ice bath and then cyclohexanecarbonyl chloride (17.5 μL, 1.1 eq, 0.13 mmol) was added. The reaction mixture was stirred at room temperature overnight. After the solvent was concentrated in vacuo, the residue was purified by chromatography (petroleum ether/acetone = 3/1) to afford **17a** as light brown solid (51 mg, 60%). M.p. 178–180 °C. ^{1}H NMR (300 MHz, $CDCl_3$): δ 1.36–1.47 (m, 2H), 1.68–1.96 (m, 8H), 2.09–2.18 (m, 1H), 3.23–3.38 (m, 2H), 3.90 (m, 3H), 5.03 (m, 2H), 5.59 (q, 1H, J = 7.8 Hz), 6.13 (d, 1H, J = 7.8 Hz), 6.93 (d, 2H, J = 8.7 Hz), 7.09 (d, 2H, J = 8.4 Hz), 7.30–7.42 (m, 8H), 7.55–7.59 (m, 2H), 7.78 (d, 1H, J = 7.5 Hz), 8.07 (d, 1H, J = 8.1 Hz), 8.13 (s, 1H), 9.42 (s, 1H). HRMS (ESI) m/z calc for $C_{40}H_{39}N_3O_5S$ $[M + H]^+$ is 674.2683, found 674.2685.

*5.1.20. (S)-Methyl 3-(2-(1-(3-(1H-indol-3-yl)propanamido)-2-(4-(benzyloxy)phenyl) ethyl)-5-phenylthiazole-4-carboxamido) benzoate (**18a**)*

Compound **18a** was prepared using similar procedures as for **20** in 88% yield for 2 steps from **16**. M.p. 77–79 °C. ^{1}H NMR (300 MHz, $CDCl_3$): δ 2.63 (t, 2H, J = 7.2 Hz), 3.09–3.13 (m, 2H), 3.89 (s, 3H), 4.99 (s, 2H), 5.52 (q, 1H, J = 8.1 Hz), 6.12 (d, 1H, J = 8.1 Hz), 6.78–6.87 (m, 5H), 7.07–7.59 (m, 14H), 7.78 (d, 1H, J = 7.8 Hz), 8.02 (d, 1H, J = 8.4 Hz), 8.13 (s, 1H), 9.31 (s, 1H). HRMS (ESI) m/z calc for $C_{44}H_{38}N_4O_5S$ $[M + H]^+$ is 735.2636, found 735.2631.

*5.1.21. (S)-3-(2-(2-(4-(Benzyloxy)phenyl)-1-(cyclohexanecarboxamido)ethyl)-5-phenylthiazole-4-carboxamido) benzoic acid (**17b**)*

To a solution of **17a** (41 mg, 1.0 eq, 0.061 mmol) in THF/MeOH/H_2O (1:1:1, 10 mL) was added $LiOH\cdots H_2O$ (26 mg, 10.0 eq, 0.61 mmol) and the solution was stirred at 50 °C for 2 h. It was diluted with CH_2Cl_2 and the water layer was acidified with 1 M HCl. The organic layer was then washed with water and brine, dried over Na_2SO_4 and concentrated in vacuo to afford acid **17b** as white solid in 99% yield. M.p. 217–219 °C. ^{1}H NMR (300 MHz, $CDCl_3$): δ 1.28–2.04 (m, 10H), 2.11–2.18 (m, 1H), 3.29–3.31 (m, 2H), 5.04 (s, 2H), 5.55 (q, 1H, J = 7.2 Hz), 6.04 (d, 1H, J = 8.1 Hz), 6.93 (d, 2H, J = 7.5 Hz), 7.09 (d, 3H), 7.28–7.56 (m, 8H), 7.82 (d, 1H, J = 8.1 Hz), 8.11 (s, 1H), 8.17 (d, 1H, J = 8.1 Hz), 9.41 (s, 1H). ^{13}C NMR (75 MHz, $CDCl_3$): δ 25.5, 25.6, 25.8, 29.4, 40.2, 45.2, 52.0, 70.1, 115.1, 121.1, 124.5, 125.7, 127.5, 128.0, 128.2, 128.6, 129.2, 129.3, 129.9, 130.2, 130.4, 131.3, 133.6, 136.9, 138.0, 141.0, 144.1, 158.0, 159.7, 168.6, 169.1, 176.7, 180.5. HRMS (ESI) m/z calc for $C_{39}H_{37}N_3O_5S$ $[M + Na]^+$ is 682.2346, found 682.2342.

*5.1.22. (S)-3-(2-(1-(3-(1H-Indol-3-yl)propanamido)-2-(4-(benzyloxy)phenyl)ethyl)-5-phenylthiazole-4-carboxamido)benzoic acid (**18b**)*

Compound **18b** was prepared using similar procedures as for **17b** in 91% yield from **18a**. M.p. 168–170 °C. ^{1}H NMR (300 MHz, $CDCl_3$): δ 2.63 (t, 2H, J = 6.9 Hz), 3.02–3.15 (m, 4H), 4.98 (s, 2H), 5.53 (q, 1H, J = 7.5 Hz), 6.18 (d, 1H, J = 8.1 Hz), 6.73–6.85 (m, 5H), 7.05–7.15 (m, 2H), 7.21 (d, 1H, J = 7.5 Hz), 7.30–7.44 (m, 7H), 7.50–7.57 (m, 3H), 7.80 (d, 1H, J = 7.5 Hz), 8.07–8.09 (m, 2H), 9.28 (s, 1H). ^{13}C NMR (75 MHz, $CDCl_3$): δ 21.4, 37.4, 40.3, 52.1, 70.2, 108.4, 111.5, 114.5, 115.2, 118.8, 119.6, 121.4, 122.2, 122.3, 123.2, 125.2, 125.9, 127.2, 127.7, 128.2, 128.4, 128.8, 129.5, 130.0, 130.4, 130.6, 136.5, 137.0,

138.3, 141.0, 143.4, 145.1, 158.0, 159.6, 163.7, 168.7, 170.5, 173.0. HRMS (ESI) *m/z* calc for $C_{43}H_{36}N_4O_5S$ $[M + Na]^+$ is 743.2299, found 743.2292.

*5.1.23. (S)-Ethyl 2-(1-(3-(1H-Indol-3-yl)propanamido)-2-(4-(benzyloxy)phenyl)ethyl)-5-phenylthiazole-4-carboxylate (**20**)*

To a solution of **3c** (1.904 g, 1.0 eq, 3.41 mmol) in CH_2Cl_2 (15 mL), trifluoroacetic acid (3 mL) was added and the mixture was stirred for 2 h at room temperature. The reaction mixture evaporated in vacuo to afford the crude amine **19**, which was used without further purification. To a solution of the amine **19** in CH_2Cl_2 (50 mL) was added 3-indolepropionic acid (0.645 g, 1.0 eq, 3.41 mmol), EDC hydrochloride (0.784 g, 1.2 eq, 4.1 mmol), DMAP (83 mg, 0.2 eq, 0.68 mmol) and Et_3N (1 mL, 2.0 eq, 6.82 mmol). The reaction mixture was stirred overnight at room temperature. The reaction mixture was extracted with ethyl acetate and the organic layer was washed successively with 1 M HCl, saturated $NaHCO_3$ and brine, dried over Na_2SO_4 and concentrated in vacuo. The crude product was purified by chromatography (petroleum ether/ethyl acetate = 1:1) to give compound **20** as white solid (1.935 g, 90% for 2 steps). ^{1}H NMR (300 MHz, $CDCl_3$): δ 1.26 (t, 3H, J = 7.2 Hz), 2.59 (t, 2H, J = 7.5 Hz), 3.07–3.22 (m, 4H), 4.28 (q, 2H, J = 7.2 Hz), 5.01 (s, 2H), 5.50 (q, 1H, J = 8.4 Hz), 6.17 (d, 1H, J = 8.1 Hz), 6.79 (d, 2H, J = 8.7 Hz), 6.88 (d, 2H, J = 8.7 Hz), 6.92 (s, 1H), 7.08–7.21 (m, 2H), 7.29–7.43 (m, 12H), 7.58 (d, 1H, J = 7.2 Hz), 8.00 (s, 1H).

*5.1.24. (S)-2-(1-(3-(1H-Indol-3-yl)propanamido)-2-(4-(benzyloxy)phenyl)ethyl)-5-phenylthiazole-4-carboxylic acid (**21**)*

To a solution of **20** (1.53 g, 1.0 eq, 2.43 mmol) in MeOH/H_2O (1:1, 50 mL) was added K_2CO_3 (1.0 g, 3.0 eq, 7.29 mmol) and the solution was stirred overnight at room temperature. It was diluted with CH_2Cl_2 and the water layer was acidified with 1 M HCl. The organic layer was then washed with water and brine, dried over Na_2SO_4 and concentrated in vacuo to afford acid **21** as white solid (1.46 g, 100%). ^{1}H NMR (300 MHz, $CDCl_3$): δ 2.58 (t, 2H), 3.00–3.15 (m, 2H), 5.01 (s, 2H), 5.47 (q, 1H, J = 8.1 Hz), 6.69–6.85 (m, 4H), 7.07–7.19 (m, 2H), 7.26–7.46 (m, 8H), 7.56 (d, 1H, J = 7.8 Hz), 7.98 (s, 1H).

*5.1.25. Compounds **18c–n** were prepared using similar procedures as for **18b** from compound **21***

*5.1.25.1. (S)-2-(2-(1-(3-(1H-Indol-3-yl)propanamido)-2-(4-(benzyloxy)phenyl)ethyl)-5-phenylthiazole-4-carboxamido)benzoic acid (**18c**).* Yield 74% for 2 steps from **21**. M.p. 190–192 °C. ^{1}H NMR (300 MHz, $CDCl_3/CD_3OD$): δ 2.51 (t, 2H), 2.96–3.01 (m, 4H), 3.73 (s, 3H), 4.92 (s, 2H), 5.59 (t, 1H), 6.70–6.77 (m, 3H), 6.98–7.49 (m, 17H), 8.14 (d, 1H, J = 7.2 Hz), 8.67 (d, 1H, J = 8.1 Hz); ^{13}C NMR (75 MHz, $CDCl_3/CD_3OD$): δ 21.1, 36.7, 38.8, 51.6, 70.0, 111.3, 113.6, 114.9, 118.3, 118.8, 120.0, 121.6, 122.1, 122.7, 126.9, 127.6, 128.0, 128.1, 128.6, 129.1, 130.2, 130.2, 130.3, 131.7, 132.6, 135.5, 135.5, 136.2, 136.8, 140.2, 142.1, 144.4, 157.6, 160.4, 167.4, 174.2. HRMS (ESI) *m/z* calc for $C_{43}H_{36}N_4O_5S$ $[M + H]^+$ is 721.2479, found 721.2480.

*5.1.25.2. (S)-4-(2-(1-(3-(1H-Indol-3-yl)propanamido)-2-(4-(benzyloxy)phenyl)ethyl)-5-phenylthiazole-4-carboxamido)benzoic acid (**18d**).* Yield 77% for 2 steps from **21**. M.p. 147–149 °C. ^{1}H NMR (300 MHz, $CDCl_3/CD_3OD$): δ 2.63 (t, 2H), 3.09–3.14 (m, 4H), 4.99 (s, 2H), 5.53 (q, 1H, J = 7.5 Hz), 6.11 (d, 1H, J = 8.4 Hz), 6.77–6.87 (m, 5H), 7.07–7.17 (m, 2H), 7.25 (d, 1H, J = 7.8 Hz), 7.31–7.59 (m, 10H), 7.69 (d, 2H, J = 8.7 Hz), 8.03 (d, 2H, J = 8.7 Hz), 9.34 (s, 1H); ^{13}C NMR (75 MHz, $CDCl_3/CD_3OD$): δ 21.3, 37.2, 39.9, 52.2, 70.0, 107.8, 111.4, 113.8, 114.9, 118.4, 118.9, 119.0, 121.7, 122.1, 125.8, 127.0, 127.5, 128.0, 128.2, 128.5, 129.3, 129.8, 130.1, 130.3, 131.0, 136.4, 136.8, 140.7, 142.0, 145.1, 157.8, 159.7, 168.5, 169.0, 173.6. HRMS (ESI) *m/z* calc for $C_{43}H_{36}N_4O_5S$ $[M + H]^+$ is 721.2479, found 721.2473.

*5.1.25.3. (S)-2-(2-(1-(3-(1H-Indol-3-yl)propanamido)-2-(4-(benzyloxy)phenyl)ethyl)-5-phenylthiazole-4-carboxamido)-6-fluorobenzoic acid (**18e**).* Yield 66% for 2 steps from **21**. M.p. 149–151 °C. ^{1}H NMR (300 MHz, $CDCl_3/CD_3OD$): δ 2.74 (t, 2H), 2.95–3.08 (m, 4H), 4.88 (s, 2H), 5.58 (m, 1H), 6.66–6.72 (m, 4H), 6.90–7.14 (m, 6H), 7.22–7.49 (m, 11H), 8.38 (d, 1H, J = 8.4 Hz); ^{13}C NMR (75 MHz, $CDCl_3/CD_3OD$): δ 21.1, 29.8, 36.6, 38.9, 51.7, 70.0, 110.9, 111.2, 111.4, 113.8, 114.9, 116.4, 118.4, 119.0, 121.8, 122.1, 122.2, 126.9, 127.7, 128.1, 128.2, 128.5, 128.7, 129.3, 130.1, 130.3, 130.4, 132.3, 136.2, 136.3, 136.9, 139.8, 141.3, 144.9, 157.7, 160.1, 160.2, 161.6, 163.6, 167.0, 167.4, 170.1, 173.9. HRMS (ESI) *m/z* calc for $C_{43}H_{35}FN_4O_5S$ $[M + Na]^+$ is 761.2204, found 761.2205.

*5.1.25.4. (S)-2-(2-(1-(3-(1H-Indol-3-yl)propanamido)-2-(4-(benzyloxy)phenyl)ethyl)-5-phenylthiazole-4-carboxamido)-5-fluorobenzoic acid (**18f**).* Yield 79% for 2 steps from **21**. M.p. 180–182 °C. ^{1}H NMR (300 MHz, $CDCl_3/CD_3OD$): δ 2.68 (t, 2H, J = 6.6 Hz), 3.07–3.26 (m, 4H), 4.97 (s, 2H), 5.48 (t, 1H, J = 6.0 Hz), 6.78 (d, 2H, J = 8.1 Hz), 6.89 (s, 1H), 6.95 (d, 2H, J = 8.4 Hz), 7.01–7.12 (m, 2H), 7.20–7.42 (m, 10H), 7.52–7.58 (m, 3H), 7.78 (dd, 1H, J = 2.7, 9.6 Hz), 8.79 (dd, 1H, J = 5.1, 9.3 Hz); ^{13}C NMR (75 MHz, $CDCl_3/CD_3OD$): δ 21.4, 37.1, 40.1, 52.2, 76.8, 111.4, 114.3, 115.0, 117.7, 118.0, 118.6, 119.2, 121.2, 121.5, 121.9, 122.1, 127.1, 127.6, 128.1, 128.2, 128.7, 128.7, 129.3, 129.6, 130.0, 130.3, 130.6, 133.2, 134.9, 135.0, 136.4, 137.0, 137.6, 141.2, 157.8, 160.1, 165.0, 167.0, 168.8, 173.4. HRMS (ESI) *m/z* calc for $C_{43}H_{35}FN_4O_5S$ $[M + H]^+$ is 739.2385, found 739.2383.

*5.1.25.5. (S)-2-(2-(1-(3-(1H-Indol-3-yl)propanamido)-2-(4-(benzyloxy)phenyl)ethyl)-5-phenylthiazole-4-carboxamido)-4-fluorobenzoic acid (**18g**).* Yield 78% for 2 steps from **21**. M.p. 240–242 °C. ^{1}H NMR (300 MHz, $CDCl_3/CD_3OD$): δ 2.53 (t, 2H), 2.98–3.00 (t, 4H), 4.88 (S, 2H), 5.52 (m, 1H), 6.58–6.71 (m, 4H), 6.89–7.16 (m, 6H), 7.26–7.48 (m, 10H), 8.06 (s, 1H), 8.54 (d, 1H); ^{13}C NMR (75 MHz, $CDCl_3/CD_3OD$): δ 21.1, 36.7, 38.9, 51.7, 70.0, 91.2, 109.3, 109.6, 111.2, 113.7, 114.8, 118.2, 118.7, 121.5, 121.9, 126.9, 127.5, 128.0, 128.1, 128.5, 128.7, 129.1, 129.9, 130.1, 130.3, 133.8, 134.9, 136.3, 136.8, 141.5, 145.0, 157.6, 160.5, 164.2, 167.5, 174.0. HRMS (ESI) *m/z* calc for $C_{43}H_{35}FN_4O_5S$ $[M + H]+$ is 739.2385, found 739.2380. HPLC purity: 98.5%.

*5.1.25.6. (S)-2-(2-(1-(3-(1H-Indol-3-yl)propanamido)-2-(4-(benzyloxy)phenyl)ethyl)-5-phenylthiazole-4-carboxamido)-4-chlorobenzoic acid (**18h**).* Yield 63% for 2 steps from **21**. M.p. 239–241 °C. ^{1}H NMR (300 MHz, $CDCl_3/CD_3OD$): δ 2.60 (t, 2H), 3.02 (t, 2H, J = 6.9 Hz), 3.13 (d, 2H, J = 6.9 Hz), 4.94 (s, 2H), 5.43 (t, 1H, J = 6.3 Hz), 6.75 (d, 2H, J = 8.1 Hz), 6.87 (s, 1H), 6.93–7.11 (m, 6H), 7.20–7.51 (m, 13H), 8.00 (d, 1H, J = 8.4 Hz), 8.82 (s, 1H). ^{13}C NMR (75 MHz, $CDCl_3/CD_3OD$): δ 21.3, 29.7, 37.0, 39.8, 52.1, 70.1, 111.3, 114.1, 114.9, 118.5, 119.0, 120.0, 121.7, 122.0, 122.9, 127.0, 127.6, 128.1, 128.2, 128.6, 128.8, 129.4, 129.9, 130.2, 130.5, 131.4, 132.8, 136.4, 136.9, 141.2, 141.9, 145.4, 157.7, 160.4, 167.2, 173.6. HRMS (ESI) *m/z* calc for $C_{43}H_{35}ClN_4O_5S$ $[M + Na]^+$ is 777.1909, found 777.1907.

*5.1.25.7. (S)-2-(2-(1-(3-(1H-Indol-3-yl)propanamido)-2-(4-(benzyloxy)phenyl)ethyl)-5-phenylthiazole-4-carboxamido)-4-bromobenzoic acid (**18i**).* Yield 63% for 2 steps from **21**. M.p. 110–113 °C. ^{1}H NMR (300 MHz, $CDCl_3$): δ 2.53 (t, 2H), 2.98 (t, 2H, J = 7.2 Hz), 3.08 (d, 2H, J = 7.2 Hz), 4.90 (s, 2H), 5.48 (t, 1H, J = 6.9 Hz), 6.72 (d, 2H, J = 8.1 Hz), 6.79 (s, 1H), 6.91–7.11 (m, 4H), 7.19 (d, 1H, J = 7.8 Hz), 7.23–7.47 (m, 12H), 8.19 (s, 1H), 8.60 (d, 1H, J = 9.0 Hz). ^{13}C NMR (75 MHz, $CDCl_3$): δ 21.3, 36.9, 38.6, 51.8, 70.0, 111.3, 113.9, 114.9, 115.2, 118.4, 119.0, 121.8, 122.0, 127.0, 127.6, 128.1, 128.2, 128.5, 128.6, 129.3, 130.0, 130.3, 130.5, 134.4, 136.0, 136.3, 136.9, 139.8, 141.6, 145.0, 157.7, 160.4, 167.3, 173.9. HRMS (ESI) *m/z* calc for $C_{43}H_{35}BrN_4O_5S$ $[M + Na]^+$ is 821.1404, found 821.1394.

*5.1.25.8. (S)-5-(2-(1-(3-(1H-Indol-3-yl)propanamido)-2-(4-(benzyloxy)phenyl)ethyl)-5-phenylthiazole-4-carboxamido)-2-fluorobenzoic acid (**18j**).* Yield 65% for 2 steps from **21**. M.p. 123–125 °C. ^{1}H NMR (300 MHz, $CDCl_3/CD_3OD$): δ 2.58 (t, 2H, J = 6.9 Hz), 3.04–3.12 (m, 4H), 4.95 (s, 2H), 5.44 (t, 1H, J = 6.3 Hz), 6.76 (d, 2H, J = 8.7 Hz), 6.84 (d, 2H), 6.99–7.10 (m, 2H), 7.21 (d, 1H, J = 7.8 Hz), 7.25–7.54 (m, 12H), 7.93–7.96 (m, 2H), 9.38 (s, 1H); ^{13}C NMR (75 MHz, $CDCl_3/CD_3OD$): δ 21.4, 29.8, 31.0, 37.1, 40.2, 52.1, 70.2, 111.5, 114.1, 115.1, 117.7, 118.6, 119.2, 122.0, 123.5, 126.4, 127.6, 128.7, 129.4, 130.2, 131.6, 132.3, 133.9, 137.0, 137.8, 140.8, 145.0, 157.0, 158.0, 160.0, 166.1, 168.8, 173.3. HRMS (ESI) m/z calc for $C_{43}H_{35}FN_4O_5S$ $[M + H]^+$ is 739.2385, found 739.2384.

*5.1.25.9. (S)-5-(2-(1-(3-(1H-Indol-3-yl)propanamido)-2-(4-(benzyloxy)phenyl)ethyl)-5-phenylthiazole-4-carboxamido)-2-chlorobenzoic acid (**18k**).* Yield 54% for 2 steps from **21**. M.p. 217–219 °C. ^{1}H NMR (300 MHz, $CDCl_3/CD_3OD$): δ 2.58 (t, 2H, J = 6.9 Hz), 3.02–3.11 (m, 4H), 4.94 (s, 2H), 6.77 (d, 2H, J = 8.7 Hz), 6.84–6.87 (m, 3H), 6.94–7.07 (m, 2H), 7.20 (d, 1H, J = 7.5 Hz), 7.29–7.53 (m, 12H), 7.78 (d, 1H, J = 8.7 Hz), 7.98 (s, 1H), 9.43 (s, 1H); ^{13}C NMR (75 MHz, $CDCl_3/CD_3OD$): δ 21.4, 29.7, 37.0, 40.1, 52.2, 70.1, 111.5, 114.0, 115.0, 118.5, 119.1, 121.9, 122.1, 122.3, 122.7, 122.8, 123.9, 127.1, 127.6, 128.1, 128.2, 128.4, 128.5, 128.6, 129.4, 129.8, 130.2, 130.4, 130.6, 131.6, 136.5, 136.6, 136.9, 140.7, 157.8, 159.7, 167.5, 173.5. HRMS (ESI) m/z calc for $C_{43}H_{35}ClN_4O_5S$ $[M + Na]^+$ is 777.1909, found 777.1905.

*5.1.25.10. (S)-3-(2-(1-(3-(1H-Indol-3-yl)propanamido)-2-(4-(benzyloxy)phenyl)ethyl)-5-phenylthiazole-4-carboxamido)-4-fluorobenzoic acid (**18l**).* Yield 58% for 2 steps from **21**. M.p. 138–140 °C. ^{1}H NMR (300 MHz, $CDCl_3$): δ 2.62 (t, 2H, J = 7.2 Hz), 3.08–3.19 (m, 4H), 5.00 (s, 2H), 5.53 (q, 1H, J = 8.4 Hz), 5.96 (d, 1H, J = 8.4 Hz), 6.79 (d, 2H, J = 9.0 Hz), 6.85 (d, 2H, J = 9.0 Hz), 6.89 (s, 1H), 7.09–7.21 (m, 2H), 7.31–7.42 (m, 9H), 7.53–7.59 (m, 2H), 7.83 (m, 1H), 7.94 (s, 1H), 9.10 (d, 1H), 9.52 (s, 1H); ^{13}C NMR (75 MHz, $CDCl_3$): δ 21.3, 22.5, 23.6, 29.7, 33.9, 37.0, 39.5, 48.2, 48.5, 48.8, 49.0, 49.3, 49.6, 52.0, 70.1, 89.1, 99.2, 111.4, 113.8, 115.0, 118.4, 119.0, 121.7, 122.1, 123.7, 127.0, 127.5, 128.0, 128.2, 128.6, 129.4, 130.2, 130.4, 130.7, 137.0, 147.1, 148.5, 157.8, 160.3, 161.4, 167.9, 173.8, 185.7. HRMS (ESI) m/z calc for $C_{43}H_{35}FN_4O_5S$ $[M + H]^+$ is 739.2385, found 739.2391.

*5.1.25.11. (S)-4-(2-(1-(3-(1H-indol-3-yl)propanamido)-2-(4-(benzyloxy)phenyl)ethyl)-5-phenylthiazole-4-carboxamido)-3-fluorobenzoic acid (**18m**).* Yield 67% for 2 steps from **21**. M.p. 212–214 °C. ^{1}H NMR (300 MHz, THF-d_8): δ 2.53 (t, 2H, J = 7.2 Hz), 3.04 (t, 2H, J = 7.5 Hz), 3.15 (dd, 1H, J = 8.4, 14.1 Hz), 3.39 (dd, 1H, J = 6.3, 14.1 Hz), 5.00 (s, 2H), 5.55 (t, 1H, J = 6.3 Hz), 6.87 (d, 2H, J = 8.4 Hz), 6.93–7.05 (m, 3H), 7.14 (d, 2H, J = 8.7 Hz), 7.22–7.40 (m, 8H), 7.54 (d, 1H, J = 7.8 Hz), 7.61 (m, 1H), 7.75–7.84 (m, 2H), 8.59 (t, 1H, J = 8.4 Hz), 9.88 (d, 1H); ^{13}C NMR (75 MHz, THF-d_8): δ 22.2, 37.7, 39.9, 53.2, 53.3, 70.6, 112.0, 115.6, 116.6, 116.9, 119.3, 119.3, 120.7, 120.8, 122.0, 122.9, 123.1, 127.4, 128.3, 128.5, 128.8, 129.2, 129.9, 130.6, 130.6, 130.7, 131.2, 138.8, 141.5, 146.3, 159.0, 160.0, 166.5, 171.8, 172.7, 172.8. HRMS (ESI) m/z calc for $C_{43}H_{35}FN_4O_5S$ $[M + Na]^+$ is 761.2204, found 761.2199.

*5.1.25.12. (S)-4-(2-(1-(3-(1H-Indol-3-yl)propanamido)-2-(4-(benzyloxy)phenyl)ethyl)-5-phenylthiazole-4-carboxamido)-2-fluorobenzoic acid (**18n**).* Yield 79% for 2 steps from **21**. M.p. 118–120 °C. ^{1}H NMR (300 MHz, $CDCl_3/CD_3OD$): δ 2.63 (t, 2H, J = 6.9 Hz), 3.02–3.13 (m, 4H), 5.00 (s, 2H), 5.48 (t, 1H, J = 6.9 Hz), 6.76–6.90 (m, 5H), 7.06–7.17 (m, 2H), 7.26–7.59 (m, 12H), 7.73 (d, 1H, J = 13.2 Hz), 7.92 (t, 1H, J = 8.4 Hz), 9.55 (s, 1H). ^{13}C NMR (75 MHz, $CDCl_3/CD_3OD$): δ 21.3, 36.9, 40.0, 52.3, 70.0, 107.4, 107.7, 111.3, 113.7, 113.9, 114.6, 114.9, 118.3, 118.8, 121.6, 122.1, 122.2, 127.0, 128.0, 128.5, 129.4, 129.7, 130.0, 130.3, 133.0, 136.4, 136.8, 140.4, 143.4, 143.6, 145.5, 157.7, 159.8, 161.2, 164.6, 166.2, 169.1, 173.7, 173.8. HRMS (ESI) m/z calc for $C_{43}H_{35}FN_4O_5S$ $[M + Na]^+$ is 761.2204, found 761.2204.

5.2. Biological assays

5.2.1. Enzyme-based assay of PTP1B

A colorimetric high throughput assay to measure inhibition against PTP1B was performed in 96-well plates. Briefly, the tested compounds were solubilized in DMSO and serially diluted into concentrations for the inhibitory test. The assays were carried out in a final volume of 100 μL containing 50 mmol/L MOPS, pH 6.5, 2 mmol/L pNPP, 30 nmol/L GST-PTP1B, and 2% DMSO, and the catalysis of pNPP was continuously monitored on a SpectraMax 340 microplate reader at 405 nm for 2 min at 30 °C. The IC_{50} value was calculated from the nonlinear curve fitting of the percent inhibition [inhibition (%)] vs the inhibitor concentration [I] using the following equation: % inhibition = $100/\{1 + (IC_{50}/[I])\ k\}$, where k is the Hill coefficient.

5.2.2. Materials

Insulin and wortmannin were obtained from Sigma Aldrich (St. Louis, MO). Radiochemical 2-deoxy-[3*H*]-deoxy-glucose, Western blotting detection kits (enhanced chemiluminescence) and Hyperfilm were purchased from Amersham Biosciences (Uppsala, Sweden).

5.2.3. Cell culture

CHO-hIR cells were cultured in Ham's F-12 medium (Invitrogen, Carlsbad, CA) supplemented with 10% (v/v) FBS, 100 units/mL penicillin and 100 μg/mL streptomycin at 37 °C in 5% CO_2. L6 myoblasts were cultured in Dulbecco's modified Eagle medium (DMEM) (Invitrogen, Carlsbad, CA) containing 10% (v/v) FBS, 4.5 g/L glucose, 100 units/mL of penicillin and 100 μg/mL streptomycin at 37 °C in 5% CO_2. For L6 myoblast differentiation, the concentration of FBS was decreased to 2%. Myotubes were used for experiments 5–7 days after differentiation.

5.2.4. Measurement of 2-deoxy-[3H]-deoxyglucose uptake in L6 myotubes

2-Deoxyglucose uptake was measured as described previously [45]. Briefly, after treatment with **18g** and subsequent stimulation with 10 nM insulin, cells were washed three times with HEPES-buffered saline solution (20 mM HEPES, 136 mM NaCl, 4.7 mM KCl, 1.25 mM $mgSO_4$, 1.2 mM $CaCl_2$, pH 7.4) followed by incubation with 2-deoxy-[3*H*]-deoxy-glucose for 15 min. Then cells were washed three times with ice-cold PBS and lysed using 0.1% Triton-X 100 and radioactivity counted.

5.2.5. Immunoblotting

CHO-hIR cells or differentiated L6 myotubes were starved in serum-free medium for 2 h. Then the cells were treated with PTP1B inhibitors for 2 h, followed by stimulation with or without 10 nM insulin for 10 min. Then cells were washed three times with ice-cold PBS and lysed with lysis buffer (50 mM Tris–HCl, pH 8.0, 150 mM NaCl, 1% NP-40, 1 mM Na_3VO_4, 1 mM PMSF, 1 mM DTT, 1 mM EDTA, 1 mM EGTA) containing complete protease inhibitors (Roche). Cell lysates were subjected to electrophoresis by 8% SDS-PAGE, electrotransferred to nitrocellulose membranes and blotted with anti-pTyr antibody from anta Cruz Biotechnology or anti-phospho-Akt (Ser473) antibody purchased from Cell Signaling Technology (Beverly, MA) and anti-β-actin antibody from Upstate (Billerica, MA). The immunoblots were visualized by chem-iluminescence using the enhanced chemiluminescence Western Blotting System.

Acknowledgments

This work was supported by The National Natural Science Foundation of China (Grants 81125023, 30725049, 30901850), the National Basic Research Program of China (Grant 2012CB524906), and the National Science and Technology Major Projects for Major New Drugs Innovation and Development (Grant 2013ZX09507002).

References

[1] J. Korner, L.J. Aronne, The emerging science of body weight regulation and its impact on obesity treatment, J. Clin. Invest. 111 (2003) 565–570.
[2] F. Ahmad, P.M. Li, J. Meyerovitch, B.J. Goldstein, Osmotic loading of neutralizing antibodies demonstrates a role for protein-tyrosine phosphatase 1B in negative regulation of the insulin action pathway, J. Biol. Chem. 270 (1995) 20503–20508.
[3] S.C. Yip, S. Saha, J. Chernoff, PTP1B: a double agent in metabolism and oncogenesis, Trends Biochem. Sci. 35 (2010) 442–449.
[4] M. Stuible, M.L. Tremblay, In control at the ER: PTP1B and the down-regulation of RTKs by dephosphorylation and endocytosis, Trends Cell Biol. 20 (2010) 672–679.
[5] W. Kaszubska, H.D. Falls, V.G. Schaefer, D. Haasch, L. Frost, P. Hessler, P.E. Kroeger, D.W. White, M.R. Jirousek, J.M. Trevillyan, Protein tyrosine phosphatase 1B negatively regulates leptin signaling in a hypothalamic cell line, Mol. Cell. Endocrinol. 195 (2002) 109–118.
[6] J.M. Zabolotny, K.K. Bence-Hanulec, A. Stricker-Krongrad, F. Haj, Y.P. Wang, Y. Minokoshi, Y.B. Kim, J.K. Elmquist, L.A. Tartaglia, B.B. Kahn, B.G. Neel, PTP1B regulates leptin signal transduction in vivo, Dev. Cell 2 (2002) 489–495.
[7] W.S. Cook, R.H. Unger, Protein tyrosine phosphatase 1B: a potential leptin resistance factor of obesity, Dev. Cell 2 (2002) 385–387.
[8] N.T. Lam, S.D. Covey, J.T. Lewis, S. Oosman, T. Webber, E.C. Hsu, A.T. Cheung, T.J. Kieffer, Leptin resistance following over-expression of protein tyrosine phosphatase 1B in liver, J. Mol. Endocrinol. 36 (2006) 163–174.
[9] K.K. Bence, M. Delibegovic, B. Xue, C.Z. Gorgun, G.S. Hotamisligil, B.G. Neel, B.B. Kahn, Neuronal PTP1B regulates body weight, adiposity and leptin action, Nat. Med. 12 (2006) 917–924.
[10] B.L. Seely, P.A. Staubs, D.R. Reichart, P. Berhanu, K.L. Milarski, A.R. Saltiel, J. Kusari, J.M. Olefsky, Protein tyrosine phosphatase 1B interacts with the activated insulin receptor, Diabetes 45 (1996) 1379–1385.
[11] D. Bandyopadhyay, A. Kusari, K.A. Kenner, F. Liu, J. Chernoff, T.A. Gustafson, J. Kusari, Protein-tyrosine phosphatase 1B complexes with the insulin receptor in vivo and is tyrosine-phosphorylated in the presence of insulin, J. Biol. Chem. 272 (1997) 1639–1645.
[12] A. Salmeen, J.N. Andersen, M.P. Myers, N.K. Tonks, D. Barford, Molecular basis for the dephosphorylation of the activation segment of the insulin receptor by protein tyrosine phosphatase 1B, Mol. Cell 7 (2001) 615–621.
[13] B.J. Goldstein, A. Bittner-Kowalczyk, M.F. White, M. Harbeck, Tyrosine dephosphorylation and deactivation of insulin receptor substrate-1 by protein-tyrosine phosphatase 1B. Possible facilitation by the formation of a ternary complex with the GRB2 adaptor protein, J. Biol. Chem. 275 (2000) 4283–4289.
[14] M.P. Myers, J.N. Andersen, A. Cheng, M.L. Tremblay, C.M. Horvath, J.P. Parisien, A. Salmeen, D. Barford, N.K. Tonks, TYK2 and JAR2 are substrates of protein-tyrosine phosphatase 1B, J. Biol. Chem. 276 (2001) 47771–47774.
[15] I.K. Lund, Mechanism of protein tyrosine phosphatase 1B-mediated inhibition of leptin signalling, J. Mol. Endocrinol. 34 (2005) 339–351.
[16] R. Di Paola, L. Frittitta, G. Miscio, M. Bozzali, R. Baratta, M. Centra, D. Spampinato, M.G. Santagati, T. Ercolino, C. Cisternino, T. Soccio, S. Mastroianno, V. Tassi, P. Al mgren, A. Pizzuti, R. Vigneri, V. Trischitta, A variation in 3′ UTR of hPTP1B increases specific gene expression and associates with insulin resistance, Am. J. Hum. Genet. 70 (2002) 806–812.
[17] S.M. Echwald, H. Bach, H. Vestergaard, B. Richelsen, K. Kristensen, T. Drivsholm, K. Borch-Johnsen, T. Hansen, O. Pedersen, A P387L variant in protein tyrosine phosphatase-1B (PTP-1B) is associated with type 2 diabetes and impaired serine phosphorylation of PTP-1B in vitro, Diabetes 51 (2002) 1–6.
[18] A. Mok, H. Cao, B. Zinman, A.J.G. Hanley, S.B. Harris, B.P. Kennedy, R.A. Hegele, A single nucleotide polymorphism in protein. tyrosine phosphatase PTP-1B is associated with protection. from diabetes or impaired glucose tolerance in ojicree, J. Clin. Endocrinol. Metab. 87 (2002) 724–727.
[19] M. Elchebly, P. Payette, E. Michaliszyn, W. Cromlish, S. Collins, A.L. Loy, D. Normandin, A. Cheng, J. Himms-Hagen, C.C. Chan, C. Ramachandran, M.J. Gresser, M.L. Tremblay, B.P. Kennedy, Increased insulin sensitivity and obesity resistance in mice lacking the protein tyrosine phosphatase-1B gene, Science 283 (1999) 1544–1548.
[20] L.D. Klaman, Increased energy expenditure, decreased adiposity, and tissue-specific insulin sensitivity in protein-tyrosine phosphatase 1B-deficient mice, Mol. Cell. Biol. 20 (2000) 5479–5489.
[21] B.A. Zinker, Reduction of protein tyrosine phosphatase 1B normalizes glucose and improves insulin sensitivity in diabetic mice, Proc. Natl. Acad. Sci. U. S. A. 99 (2002) 11357–11362.
[22] C.M. Rondinone, J.M. Trevillyan, J. Clampit, R.J. Gum, C. Berg, P. Kroeger, L. Frost, B.A. Zinker, R. Reilly, R. Ulrich, M. Butler, B.P. Monia, M.R. Jirousek, J.F. Waring, Protein tyrosine phosphatase 1B reduction regulates adiposity and expression of genes involved in lipogenesis, Diabetes 51 (2002) 2405–2411.
[23] T.O. Johnson, J. Ermolieff, M.R. Jirousek, Protein tyrosine phosphatase 1B inhibitors for diabetes, Nat. Rev. Drug Discov. 1 (2002) 696–709.
[24] S. Zhang, Z. Zhang, PTP1B as a drug target: recent developments in PTP1B inhibitor discovery, Drug Discov. Today 12 (2007) 373–381.
[25] R.H. van Huijsduijnen, A. Bombrun, D. Swinnen, Selecting protein tyrosine phosphatases as drug targets, Drug Discov. Today 7 (2002) 1013–1019.
[26] A.J. Barr, Protein tyrosine phosphatases as drug targets: strategies and challenges of inhibitor development, Future Med. Chem. 2 (2010) 1563–1576.
[27] A.P. Combs, Recent advances in the discovery of competitive protein tyrosine phosphatase 1B inhibitors for the treatment of diabetes, obesity, and cancer, J. Med. Chem. 53 (2010) 2333–2344.
[28] V.V. Vintonyak, H. Waldmann, D. Rauh, Using small molecules to target protein phosphatases, Bioorg. Med. Chem. 19 (2011) 2145–2155.
[29] S. Thareja, S. Aggarwal, T.R. Bhardwaj, M. Kumar, Protein tyrosine phosphatase 1B inhibitors: a molecular level legitimate approach for the management of diabetes mellitus, Med. Res. Rev. 32 (2012) 459–517.
[30] D. Popov, Novel protein tyrosine phosphatase 1B inhibitors: interaction requirements for improved intracellular efficacy in type 2 diabetes mellitus and obesity control, Biochem. Biophys. Res. Commun. 410 (2011) 377–381.
[31] Y. Wei, Y.-T. Chen, L. Shi, L.-X. Gao, S. Liu, Y.-M. Cui, W. Zhang, Q. Shen, J. Li, F.-J. Nan, Discovery and structural modification of novel inhibitors of PTP1B inspired by the ACT fragment of scleritodermin A, Med. Chem. Commun. 2 (2011) 1104–1109.
[32] E.W. Schmidt, C. Raventos-Suarez, M. Bifano, A.T. Menendez, C.R. Fairchild, D.J. Faulkner, Scleritodermin A, a cytotoxic cyclic peptide from the lithistid sponge Scleritoderma nodosum, J. Nat. Prod. 67 (2004) 475–478.
[33] K.E. YouTen, E.S. Muise, A. Itie, E. Michaliszyn, J. Wagner, S. Jothy, W.S. Lapp, M.L. Tremblay, Impaired bone marrow microenvironment and immune function in T cell protein tyrosine phosphatase-deficient mice, J. Exp. Med. 186 (1997) 683–693.
[34] A. Fukushima, K. Loh, S. Galic, B. Fam, B. Shields, F. Wiede, M.L. Tremblay, M.J. Watt, S. Andrikopoulos, T. Tiganis, T-cell protein tyrosine phosphatase attenuates STAT3 and insulin signaling in the liver to regulate gluconeogenesis, Diabetes 59 (2010) 1906–1914.
[35] T. Tiganis, PTP1B and TCPTP-nonredundant phosphatases in insulin signaling and glucose homeostasis, FEBS J. 280 (2013) 445–458.
[36] A.R. Saltiel, C.R. Kahn, Insulin signalling and the regulation of glucose and lipid metabolism, Nature 414 (2001) 799–806.
[37] N.J. Bryant, R. Govers, D.E. James, Regulated transport of the glucose transporter GLUT4, Nat. Rev. Mol. Cell Biol. 3 (2002) 267–277.
[38] G. Powis, R. Bonjouklian, M.M. Berggren, A. Gallegos, R. Abraham, C. Ashendel, L. Zalkow, W.F. Matter, J. Dodge, G. Grindey, C.J. Vlahos, Wortmannin, a potent and selective inhibitor of phosphatidylinositol-3-kinase, Cancer Res. 54 (1994) 2419–2423.
[39] D. Barford, A.J. Flint, N.K. Tonks, Crystal structure of human protein tyrosine phosphatase 1B, Science 263 (1994) 1397–1404.
[40] K. Kolmodin, J. Åqvist, The catalytic mechanism of protein tyrosine phosphatases revisited, FEBS Lett. 498 (2001) 208–213.
[41] Z.C. Jia, D. Barford, A.J. Flint, N.K. Tonks, Structural basis for phosphotyrosine peptide recognition by protein tyrosine phosphatase 1B, Science 268 (1995) 1754–1758.
[42] Y.A. Puius, Y. Zhao, M. Sullivan, D.S. Lawrence, S.C. Almo, Z.Y. Zhang, Identification of a second aryl phosphate-binding site in protein-tyrosine phosphatase 1B: a paradigm for inhibitor design, Proc. Natl. Acad. Sci. U. S. A. 94 (1997) 13420–13425.
[43] G. Liu, Z.L. Xin, H. Liang, C. Abad-Zapatero, P.J. Hajduk, D.A. Janowick, B.G. Szczepankiewicz, Z.H. Pei, C.W. Hutchins, S.J. Ballaron, M.A. Stashko, T.H. Lubben, C.E. Berg, C.M. Rondinone, J.M. Trevillyan, M.R. Jirousek, Selective protein tyrosine phosphatase 1B inhibitors: targeting the second phosphotyrosine binding site with non-carboxylic acid-containing ligands, J. Med. Chem. 46 (2003) 3437–3440.
[44] D. Sellanes, E. Manta, G. Serra, Toward the total synthesis of Scleritodermin A: preparation of the C-1-N-15 fragment, Tetrahedron Lett. 48 (2007) 1827–1830.
[45] L.P. Xie, S.Y. Lee, J.N. Andersen, S. Waters, K. Shen, X.L. Guo, N.P.H. Moller, J.M. Olefsky, D.S. Lawrence, Z.Y. Zhang, Cellular effects of small molecule PTP1B inhibitors on insulin signaling, Biochemistry 42 (2003) 12792–12804.